CHAPTER 4

Room acoustics

4.1 INTRODUCTION

In talking about the concept of room acoustics we shall include all aspects of the behaviour of sound in a room, covering both the physical aspects as well as the subjective effects. In other words, room acoustics deals with measurement and prediction of the sound field resulting from a given distribution of sources as well as how a listener experiences this sound field, i.e. will the listener characterize the room as having "good acoustics"? When designing for a good acoustic environment, which could be everything from introducing some absorbers into an office space to the complete design of a concert hall, one must bear in mind both the physical and the psychological aspects. This implies having knowledge on how the shape of the room, the dimensions and the material properties of the construction influences the sound field. Just as important, however, is a knowledge of the relationship between the physical measurable parameters of this field and the subjective impression for a listener. Finding such objective parameters, either measurable or predictable, which correlate well with the subjective impression of the acoustic quality, is still a subject of research. It goes without saying that the number of suggested parameters is quite large. The reverberation time in a room has been, and still is, an important parameter in any judgement of quality. Another large group of parameters are also based on the impulse responses of the room but here the emphasis is on the relative energy content in given time intervals.

In this chapter, the primary emphasis will be on the physical properties, partly to give a background for the most common measurement methods in room acoustics. Suggested requirements for parameters, other than the reverberation time, will to some extent also be touched on.

4.2 MODELLING OF SOUND FIELDS IN ROOMS. OVERVIEW

In principle, we should be able to calculate the sound field in a room, generated by one or more sources, applying a wave equation of the same type as used earlier in the one-dimensional case (see section 3.6). There we introduced a sound source as a mass flux q, having the dimensions of $\mathrm{kg \cdot m^{-3} \cdot s^{-1}}$, in the equation of continuity. In the three-dimensional case, we obtain

$$\nabla^2 p - \frac{1}{c_0^2} \cdot \frac{\partial^2 p}{\partial t^2} + \frac{\partial q}{\partial t} = 0. \qquad (4.1)$$

Solving this equation analytically will normally become very difficult except for simple room shapes and simple boundary conditions, e.g. an empty rectangular-shaped room

having walls of infinite stiffness. Solutions for such special cases may, however, give some general information on sound fields in rooms. It is therefore useful to discuss some of these cases, which we shall return to in section 4.4.2.

The development of numerical techniques in recent time has been formidable, which include FEM (finite element methods), BEM (boundary element methods) and various other numerical methods for predicting sound propagation in bounded spaces. Using these, accurate solutions may be obtained for complex room shapes and boundary conditions. First and foremost, these techniques are suitable in the lower frequency ranges, i.e. when the ratio between a typical room dimension and the wavelength is not too large. When using a FEM technique a reasonable number of elements per wavelength are of the order three to four. If the typical room dimension is 10 metres one may at 100 Hz perhaps use 1000 elements. However, to calculate with the same accuracy at 1000 Hz one needs 1000000 elements. Depending on the specific computer FEM software, different types of elements are implemented, having some 8 to 20 nodes. At each of these nodes we shall then calculate the sound field quantity in question. In spite of the large capacity of modern computers, the limitations imposed on these calculations should be obvious. It should, however, be stressed that FEM calculations have become very important tools in the area of sound radiation and sound transmission, in particular where a strong coupling between a vibrating structure and the surrounding medium is expected.

A number of other approximate methods have a long history in room acoustics. The reason is that one normally is not interested in a detailed description frequency by frequency. The average value in frequency bands, being either octave or one-third-octave bands, has been more relevant. In the literature one will therefore find methods characterized under headings such as *statistical room acoustics* and *geometrical room acoustics.* The first term implies treating the sound pressure in a room as a stochastic quantity with a certain space variance. The classical *diffuse field* model, also called the *Sabine* model, is an extreme case in this respect. The latter name is a recognition of the American scientist Wallace Clement Sabine (1868–1919) who published his famous article “Reverberation” in the year 1900 containing a formula for the reverberation time in rooms, a formula still being the most used. In a diffuse field model, the space variance of the sound pressure is zero, the energy density is everywhere the same in the room. Such a model may be seen as the acoustic analogue of the classical kinetic gas model.

There is also a long tradition for using geometrical models in acoustics, see e.g. Pierce (1989). For geometrical acoustics in general, also denoted ray acoustics, the concept of *wave front* is central. At a given frequency, a wave front is a surface where the sound pressure everywhere is in phase. As the wave front moves in time, the line described in space by a given point on the surface is called the *ray path.* Generally, it is not necessary to assume that the amplitude is constant over the wave front or that the wave front is a plane surface but in room acoustics this is assumed. Curved paths have no place in geometrical room acoustics; the sound energy propagates along straight ray paths just like light. Inherent in these geometrical models there is no frequency information and the validity of the calculated results is in principle limited to a frequency range where we may assume specular reflections and where diffraction phenomena may be neglected. Such phenomena may, however, be included in these models by certain artifices. We shall deal with them by giving an overview of the principles.

4.2.1 Models for small and large rooms

We have given an overview and some general remarks concerning the different models used to predict the sound field in rooms. We shall proceed by going into more detail on the suitability of these models for given situations. Simple diffuse field models may in practice be quite sufficient predictors given that a certain minimum number of room modes are being excited and participate in the build-up of the sound field. However, there are also a number of other conditions that have to be fulfilled before it is reasonable to assume that a global sound pressure level or a global reverberation time exists. The linear dimensions of the room must not be too different; the absorption material must be reasonably evenly distributed on the room surfaces and the total absorption area must not be too high.

To apply the simple expressions for the reverberation time, given in section 4.5.1.2 below, also presupposes that only the room volume and the total surface area determine the *mean free path* of the sound, i.e. the distance between each reflection. When filling the room with a certain number of scattering objects an "internal" reverberation process may be set up between these objects and the common reverberation time formulae are no longer applicable. We should then bear in mind how to explain the diffusing elements required for laboratories performing standard absorption measurements according to ISO 354. We shall return to this question when treating the subject of scattering.

In conclusion, large discrepancies between the ideal conditions demanded for a diffuse field and the actual room conditions make such models unsuitable. It may be that the linear dimensions are quite different; e.g. the room is "flat" in the sense that the ceiling height is small compared to the length and width of the room (industrial hall, landscaped office etc.) or the room is "long" (a corridor etc.). Absorbing materials or objects may also be unevenly distributed and the room may also contain a number of different types of reflecting and/or scattering object.

The choice of models to use on such "large rooms" is obviously dependent on the intended function for the room, a function that also determines the parameters we shall use to validate the acoustic quality. On industrial premises, e.g. large industrial halls, where a large attenuation between the various noise sources and the workers is aimed at, the decrease in decibels per metre distance may be a suitable parameter to estimate. For rooms having a simple shape, such a parameter could be estimated by an analytical model.

In performance spaces, theatres, auditoria, concert halls etc., the function of the room is to forward the sound to the audience, which implies that a quite different set of parameters, are necessary. Predicting the sound field in such rooms is generally based on methods from geometrical acoustics, partly combined with statistical considerations to include scattering (diffusion) phenomena. Two methods, principally different, are used: the ray-tracing method and the mirror-source method. The former simulates a sound source by emitting a large number of "sound rays", these being evenly distributed over the solid angle covered by the actual sound source. Each ray is followed as it hits the various surfaces in the room, being specularly reflected and radiated having a reduced energy caused by the absorption factor of the surface.

According to the name, the mirror-source method is based on the mirror images of the real source. The sound from a mirror source received at a given point is reflected *once* in the surface of the mirror. These first-order sources are then being mirrored by all room surfaces giving second-order sources and so on. Short descriptions of these two geometrical prediction models are given in section 4.8. Software having implemented these methods is commercially available. Most of them are based on a hybrid method

combining the principles outlined above. A number of them have the possibility of simulating simple types of scattering effect.

4.3 ROOM ACOUSTIC PARAMETERS. QUALITY CRITERIA

The parameters used for assessing the acoustic quality of a room obviously depend on its intended use. Whereas the reverberation time and/or the sound level reduction by distance from the source may be sufficient in an industrial hall, a more comprehensive set of parameters must be used in e.g. concert halls. It is acknowledged that the reverberation time has an important role and there is sufficient background experience on how long or short it should be depending on the size of the room and related to the type of the performance room; theatre, room for music performance etc. As for music performance, the type of music will be a vital factor; see e.g. Kuttruff (1999).

A number of other parameters that correlates well with the subjective impression are based on data calculated from measured impulse responses in the room; see ISO 3382. An example is shown in Figure 4.1, a measured impulse response using an MLS technique (see section 1.5.2).

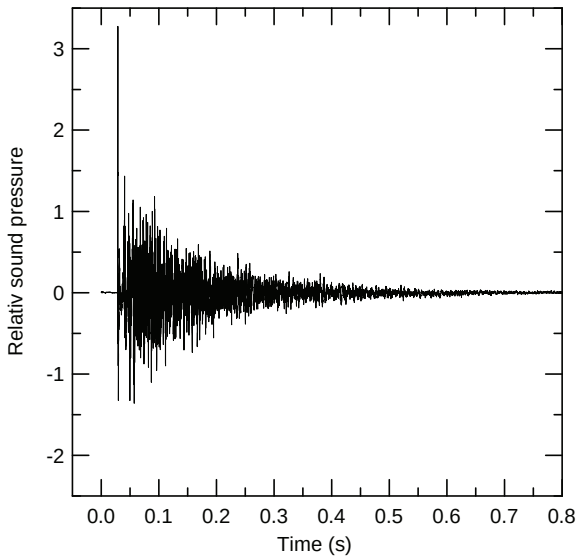

Figure 4.1 A measured impulse response in an 1800 m^3 auditorium using a MLS signal (sequence length of order 16 and sampling frequency 25 kHz of which only every second point is shown). After Lundeby et al. (1995).

Irrespective of the intended use of the room, whether for speech or music, it is important to design the room in such a way as to give a balanced set (in time) of the early reflections onto the audience area. Reflections following the direct sound within a time span of approximately 50 milliseconds will contribute to the strength of the direct sound. A listener will not perceive these reflections as a separate part or as an echo, but will if a strong reflection has a longer delay. This phenomenon is called the *precedence effect* or

Haas effect, the latter name in recognition of one of the many researchers on the phenomenon, Haas (1951).

Added to the time arrival of the reflections, it is important for rooms for music performances to know *where* the reflections are coming from. The directional distribution is critical for the listener's feeling of spaciousness of the sound field, i.e. lateral reflections are just as important as reflections from the ceiling. Added to this fact, there has in the last 20 years been a growing awareness that diffuse reflections are also very important, again for rooms for music performances. We shall therefore give some examples of these other objective acoustic parameters used for larger halls, how they are determined and, to a limited extent, on the underlying subjective matter.

4.3.1 Reverberation time

The reverberation time T is defined as the time required for the sound pressure level in a room to decrease by 60 dB from an initial level, i.e. the level before the sound source is stopped. This is not necessarily coincident with a listeners feeling of reverberation and in ISO 3382 one will find that measurement of the *early decay time* (EDT) is recommended as a supplement to the conventional reverberation time. Both parameters are determined from the *decay curve*, EDT from the first 10 dB of decay, and T normally from the 30 dB range between –5 and –35 dB below the initial level. Both quantities are calculated as the time necessary for a 60 dB decay having the rate of decay in the ranges indicated.

Throughout the time a number of methods have been used to determine the decay curves and thereby the reverberation time. A common method is to excite the room by a source emitting band limited stochastic noise, which is turned off after a constant sound pressure level is reached. For historical reasons, we shall mention the so-called level recorders, a level versus time writer, recording directly the sound pressure level decay, where the eye could fit a straight line. Later developments included instruments giving out the decay data digitally, enabling a line fit e.g. by the method of least squares.

Modern methods based on deterministic signals such as MLS or SS, however, are superior in the dynamic range achieved in the measurements and may well measure over a decay range of 60 dB or more. It may be shown that the decay curve is obtained by a "backward" or reversed time integration of impulse responses as the one shown in Figure 4.1. Normally as we are interested in the reverberation as a function of frequency, the impulse response is filtered in octave or one-third-octave bands before performing this integration. The decay as a function of time is then given by

$$E(t) = \int_t^\infty p^2(\tau)\,\mathrm{d}\tau = \int_\infty^t p^2(\tau)\,\mathrm{d}(-\tau), \tag{4.2}$$

where p is the impulse response. Certainly, this equation was also utilized when analogue measuring equipment was used by splitting the integral into two parts as follows

$$E(t) = \int_t^\infty p^2(\tau)\,\mathrm{d}\tau = \int_0^\infty p^2(\tau)\,\mathrm{d}\tau - \int_0^t p^2(\tau)\,\mathrm{d}\tau. \tag{4.3}$$

The upper limit of the integration poses a problem as the background noise unrelated to the source signal will be integrated as well. Different techniques are suggested to minimize the influence of background noise. One method is to estimate the background

noise from the later part of the impulse response, thereafter compensating for the noise by assuming that the energy decays exponentially with the same decay rate as the actual one at a level 10–15 dB above the background level. Such a technique (see Lundeby et al. (1995)) is used calculating the decay curves shown in Figure 4.2. The impulse response shown in Figure 4.1 is filtered by a one-third-octave band of centre frequency 1000 Hz and the decay curves are calculated with and without being compensated for background noise. In one set of curves, the level of the background is equal to the one present at the time of measurement. In the second set, the background noise is artificially increased to show that also in this case one will obtain a decay curve having an acceptable dynamic range. Ideally, all the solid curves should be coincident but this will only be the case if the decay rate is everywhere the same.

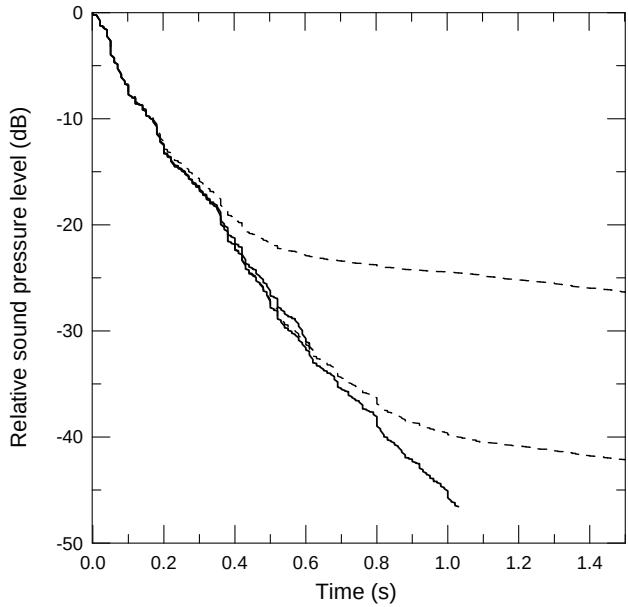

Figure 4.2 Decay curves based on filtering, one-third-octave band 1000 Hz and reverse time integration of the impulse response shown in Figure 4.1. Solid curves – integration with background noise compensation. Dashed curves – integration of the total impulse response. One set of curves is using an artificially added noise. After Vigran et al. (1995).

4.3.2 Other parameters based on the impulse response

A large number of parameters suggested in the literature and applied over the years are listed and commented on in ISO 3382. These are all derived from measured impulse responses, and we shall present a selection of these measures.

The balance between the early and late arriving sound energy, which concerns the balance between the clarity (or distinctness) and the feeling of reverberation, is important for music as well as for speech. Several parameters are suggested to cover this matter in room acoustics. The simplest ones deal with the ratio of the total sound energy received

in the first 50 or 80 milliseconds to the rest of the energy received. We have an *early-to-late index* C_{te} defined by

$$C_{t_e} = 10 \cdot \lg\left(\int_0^{t_e} p^2(t)\,\mathrm{d}t \Big/ \int_{t_e}^{\infty} p^2(t)\,\mathrm{d}t \right), \tag{4.4}$$

where t_e is 50 ms for speech and 80 ms for music. A recommended value for this parameter is 0 dB.

An early variant of this parameter was D_{50}, which is denoted *definition* in line with the original German notion of *Deutlichkeit.* The difference from the above is that, instead of the late energy, one is using the total energy received. Hence

$$D_{50} = \int_0^{50\mathrm{ms}} p^2(t)\,\mathrm{d}t \Big/ \int_0^{\infty} p^2(t)\,\mathrm{d}t. \tag{4.5}$$

The relationship between C_{50} and D_{50} is then given by

$$C_{50} = 10 \cdot \lg\left(\frac{D_{50}}{1 - C_{50}} \right), \tag{4.6}$$

making it unnecessary to measure both parameters.

By way of introduction, we pointed out that the direction of sound incidence was important for the feeling of spaciousness. Of special importance are the lateral reflections, which also contribute to an impression of widening a source or a source area. Several early lateral energy measures are proposed, one is the *lateral energy fraction LF* based on measured impulse responses obtained from an omni-directional and a figure-of-eight pattern microphones. It is defined as

$$LF = \int_{5\mathrm{ms}}^{80\mathrm{ms}} p_{\mathrm{L}}^2(t)\,\mathrm{d}t \Big/ \int_0^{80\mathrm{ms}} p^2(t)\,\mathrm{d}t, \tag{4.7}$$

where p_{L} is the sound pressure obtained with the figure-of-eight microphone. This microphone is intended to be directed in such a way that it responds predominantly to sound arriving from the lateral directions and is not significantly influenced by the direct sound.

Because the directivity of a figure-of-eight microphone essentially has a cosine pattern and the pressure is squared, the resulting contribution from a given reflection will vary with the square of the cosine of the angle between the reflection relative to the axis of maximum sensitivity of the microphone. An alternative parameter is *LFC*, where the contributions will be a function of the cosine to this angle. This parameter, which is believed to be subjectively more accurate, is defined by

$$LFC = \int_{5\mathrm{ms}}^{80\mathrm{ms}} \left| p_{\mathrm{L}}(t) \cdot p(t) \right| \mathrm{d}t \Big/ \int_0^{80\mathrm{ms}} p^2(t)\,\mathrm{d}t. \tag{4.8}$$

In addition to the parameters given above, there are others related to our binaural hearing, based on measurements using an artificial or dummy head. These so-called *inter-aural cross correlation* measures are correlated to the subjective quality of "spatial impression".

4.4 WAVE THEORETICAL MODELS

Obtaining analytical solutions to the wave equation (4.1) are difficult except in cases where the room has a simple shape and simple boundary conditions. In section 3.6, we arrived at a solution for the sound field in a simple one-dimensional case: a tube closed in both ends and with stiff walls where we assumed that the particle velocity everywhere was equal to zero. We may easily generalize these results to the three-dimensional case if we assume that the room has a rectangular shape with dimensions L_x, L_y and L_z. We shall use this as an example to illustrate some important properties of sound fields in rooms; how the impulse response will depend on e.g. the room dimensions and furthermore, how we may predict the impulse responses.

For a free wave field we shall have to solve the wave equation without the source term. Assuming harmonic time dependence, we get the Helmholtz equation for the sound pressure in three-dimensional form

$$\nabla^2 p + k^2 p = 0, \tag{4.9}$$

where k is the wave number. Initially, we shall assume that all boundary surfaces are infinitely stiff and there are no other energy losses in the room. The eigenfunctions for the pressure will then be given by

$$p_{n_x n_y n_z}(x, y, z) = C \cdot \cos(k_x x) \cdot \cos(k_y y) \cdot \cos(k_z z), \tag{4.10}$$

where C is a constant and where the eigenvalues for the wave number is given by

$$k_n^2 = k_x^2 + k_y^2 + k_z^2 = \left(\frac{n_x \pi}{L_x}\right)^2 + \left(\frac{n_y \pi}{L_y}\right)^2 + \left(\frac{n_z \pi}{L_z}\right)^2. \tag{4.11}$$

The corresponding eigenfrequencies are given by

$$f_{n_x n_y n_z} = \frac{c_0}{2}\left[\left(\frac{n_x}{L_x}\right)^2 + \left(\frac{n_y}{L_y}\right)^2 + \left(\frac{n_z}{L_z}\right)^2\right]^{\frac{1}{2}}. \tag{4.12}$$

To each of these eigenfunctions or normal modes there is a set of numbers, a set of indices. Equation (4.10) then represents a three-dimensional standing wave if we multiply with the time-dependent factor $\exp(j\omega t)$. In the literature special names are used for the wave forms associated with these sets of indices. We have an *axial mode* when two of the indices are equal to zero, a *tangential mode* when just one of the indices is zero, and finally, an *oblique mode* when all indices are different from zero. (Can you tell the direction of the wave in the room in these three cases?)

For the case of the one-dimensional standing wave, we named the points where the sound pressure was zero as *nodal points*. By analogy, here we shall have *nodal planes* if one or more of these indices is zero and the indices will indicate the number of such planes normal to the x-, y- and z-axis, respectively. That the nodal points have the form of a plane is a special case due to the example we have chosen, the rectangular room. For other shapes we shall have other types of geometric surface; we shall call them *nodal surfaces*.

4.4.1 The density of eigenfrequencies (modal density)

Concerning measurements in building acoustics, such as sound insulation, sound absorption, sound power etc. the eigenfrequencies per se are not particularly important. The relative density, i.e. the number of eigenfrequencies within a given bandwidth, is, however, of crucial importance for measurement accuracy. By analogy to the calculation of the modal density for a plate (see section 3.7.3.5), we may develop a wave number diagram having the shape as the octant of a sphere. Summing up the number of "points" or eigenfrequencies N below a given frequency f, we arrive at the following approximate expression

$$N \approx \frac{4\pi f^3}{3c_0^3} \cdot V + \frac{\pi f^2}{4c_0^2} \cdot S + \frac{Lf}{8c_0}, \tag{4.13}$$

where V, S and L are the room volume, the total surface area of the room and the total length of the edges, respectively. Differentiating this expression with respect to frequency we arrive at the following approximate expression for the modal density

$$\frac{\Delta N}{\Delta f} \approx \frac{4\pi f^2}{c_0^3} \cdot V + \frac{\pi f}{2c_0^2} \cdot S + \frac{L}{8c_0}. \tag{4.14}$$

As seen, the first term will be the dominant one at higher frequencies, and in the literature one often finds this term alone. This certainly has the advantage of requiring the room volume only, but this practice may introduce large errors at low frequencies.

Example An ordinary sitting room in a dwelling with dimensions $L_x \cdot L_y \cdot L_z$ equal to $6.2 \cdot 4.1 \cdot 2.5$ metres, gives us a floor area of 25.4 m^2 and a volume of 63.6 m^3. Choosing a frequency of 100 Hz, Equation (4.14) gives us $\Delta N/\Delta f$ equal to 0.361. If we measure using one-third-octave bands filters, at centre frequency 100 Hz we get a bandwidth $\Delta f \approx 0.23 \cdot 100 = 23$ Hz. We will then get $23 \cdot 0.361 \approx 8$ eigenfrequencies inside this band, which compares well with an exact calculation giving seven eigenfrequencies. If we just use the first term we will get five eigenfrequencies. However, going up in frequency the first term will become dominant. Keeping a fixed bandwidth of 23 Hz and moving up to 1000 Hz, we expect to find approximately 500 eigenfrequencies (the first term alone gives 470). Using a one-third-octave filter we arrive at approximately 5000 eigenfrequencies inside the band.

4.4.2 Sound pressure in a room using a monopole source

We shall proceed by calculating the sound field in a room of rectangular shape where we have placed a sound source in a given position. This is again a generalization of the one-dimensional case of a tube with a sound source (see section 3.6). We shall assume that the source is a monopole, pulsating harmonically in time. The task is then to solve the Helmholtz equation (4.9) but now modified with a source term on the right side of the equation. We shall characterize the monopole source by its volume velocity or source strength Q having unit m^3/s, i.e. not by the mass q as in Equation (4.1). The pressure root-mean-square-value in a given point (x,y,z) caused by the source in a position (x_0,y_0,z_0) may be written

$$\tilde{p}(x,y,z) = \rho_0 c_0^2 \tilde{Q} \sum_{n_x=0}^{\infty} \sum_{n_y=0}^{\infty} \sum_{n_z=0}^{\infty} \frac{\omega \cdot \Psi_{n_x n_y n_z}(x,y,z) \cdot \Psi_{n_x n_y n_z}(x_0,y_0,z_0)}{V_{n_x n_y n_z}\left(\omega^2 - \omega_{n_x n_y n_z}^2\right)}. \quad (4.15)$$

The quantity ω is the angular frequency of the source, and $\omega_{n_x n_y n_z}$ are the eigenfrequencies according to Equation (4.12). The Ψ-functions are the corresponding eigenfunctions:

$$\Psi_{n_x n_y n_z}(x,y,z) = \cos\frac{n_x \pi x}{L_x} \cdot \cos\frac{n_y \pi y}{L_y} \cdot \cos\frac{n_z \pi z}{L_z}. \quad (4.16)$$

$V_{n_x n_y n_z}$ is a normalizing factor, depending on the modal numbers, given by

$$V_{n_x n_y n_z} = V \cdot \varepsilon_{n_x} \cdot \varepsilon_{n_y} \cdot \varepsilon_{n_z}, \quad \text{where} \quad \varepsilon_n = 1 \text{ for } n = 0 \quad \text{and} \quad \varepsilon_n = \frac{1}{2} \text{ for } n \geq 1. \quad (4.17)$$

The equations are derived assuming no energy losses in the room. However, as shown earlier in section 3.7.3.6, we may introduce small losses by complex eigenfunctions. We shall write

$$\bar{\omega}_{n_x n_y n_z} = \omega_{n_x n_y n_z} \sqrt{1 + \mathrm{j} \cdot \eta} = \omega_{n_x n_y n_z} \sqrt{1 + \mathrm{j} \cdot \frac{4.4 \cdot \pi}{\omega_{n_x n_y n_z} \cdot T}}, \quad (4.18)$$

where η is the loss factor and T the corresponding reverberation time. As an example of the use of Equation (4.15), we shall calculate the pressure at a given position in the same room as used in the example in section 4.4.1. We shall make the reverberation time 1.0 seconds independent of frequency.

The pressure response is shown in Figure 4.3 represented by the transfer function $p/(Q \cdot \omega)$ on a logarithmic scale for a frequency range up to 1000 Hz. This implies that we have related the pressure to the volume acceleration of the monopole source, both given by their root-mean-square-values. Also shown in the diagram are the lowest 10 eigenfrequencies. It will appear that only the very low frequency resonances may be identified. In the higher frequency range we find that the response is made up by contributions from many modes.

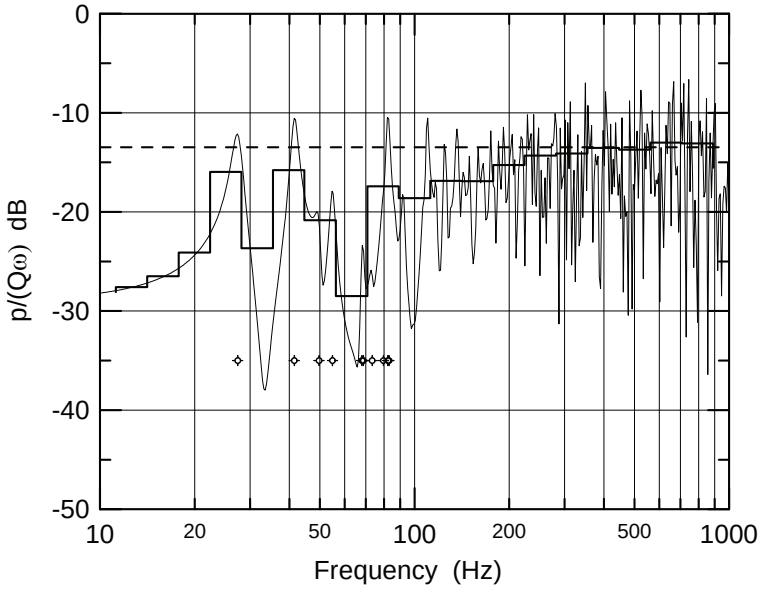

Figure 4.3 Transfer function between sound pressure and monopole source volume acceleration in a room of dimensions 6.2 x 4.1 x 2.5 metres and reverberation time 1.0 seconds. Source position (1.7, 1.0, 1.5), receiver position (3.5, 2.5, 1.5). Thick solid curve – analysis in one-third-octave bands. Dashed line – diffuse-field model. The points show calculated resonance frequencies.

The response is also shown resulting from an analysis in one-third-octave bands, a normal procedure when performing measurements in buildings. It is then of interest to calculate the result if one is using a simple diffuse field model for this case (see section 4.5.1 below). Assuming that the pressure at the receiver position is not affected by the direct field from the source, we may use the simple relationship between the source power W and the average sound pressure in the room stating that

$$W = \frac{\tilde{p}^2}{4\rho_0 c_0} \cdot A = \frac{\tilde{p}^2}{4\rho_0 c_0} \cdot \frac{55.3 \cdot V}{c_0 T}, \tag{4.19}$$

where A is the total absorbing area in the room. A monopole source freely suspended in the room will radiate a power

$$W_{\text{monopole}} = \frac{\rho_0 c_0 k^2 \tilde{Q}^2}{4\pi}. \tag{4.20}$$

Equating these powers, we obtain

$$\frac{\tilde{p}}{\tilde{Q}\omega} = \rho_0 \sqrt{\frac{c_0 T}{55.3\pi V}}. \tag{4.21}$$

The result is shown by the dashed line in Figure 4.3. We see that there is a good fit between this result and the frequency averaged data in the frequency range above 200 Hz. However, it must be noted that we have performed a calculation just for one receiver position. Determining the emitted power from a source in a standard reverberation room test (see ISO 3741) the squared sound pressure is space averaged by using a number of microphone positions. It is interesting to note that this standard requires a minimum room volume of 70 m^3 (the volume in our example is approximately 64 m^3) permitting measurements upwards from 200 Hz.

4.4.3 Impulse responses and transfer functions

The common measurement procedure today is to determine pertinent impulse responses, hereby using these to calculate reverberation time, other room acoustic measures and transfer functions if required. In the preceding section, we calculated the transfer function between the sound pressure at a given position in a room and the volume acceleration of a source at another position. Vice versa, by an inverse Fourier transform of the transfer function we shall arrive at the impulse response, from which we may calculate the reverberation time and check that it is correct. The latter means that it is 1.0 second independent of frequency, as presupposed when calculating the transfer function shown in Figure 4.3.

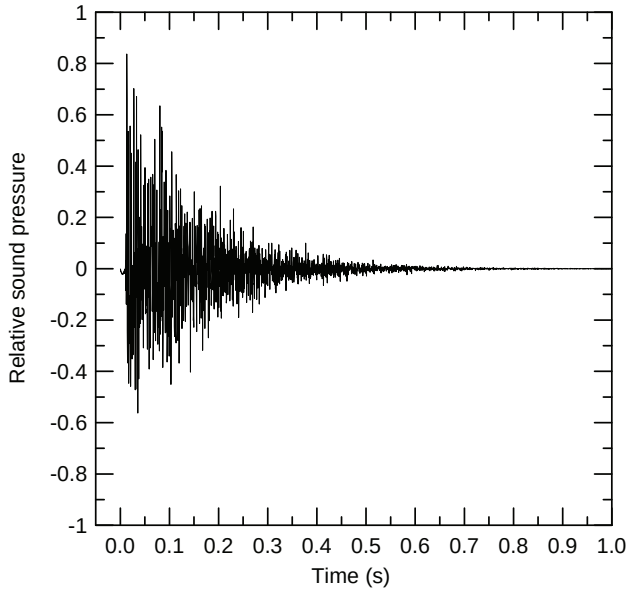

Figure 4.4 Impulse response calculated from the transfer function shown in Figure 4.3.

The unfiltered impulse response (for the frequency range up to 1000 Hz) corresponding to the transfer function in Figure 4.3 is shown in Figure 4.4. It should be noted that when calculating the inverse transform one must ensure that the result, the impulse response, turns out to be a purely real quantity, which implies a meticulous treatment of the real and imaginary part of the transfer function.

The unfiltered impulse response may now be filtered in either octave or one-third-octave bands to arrive at the reverberation time in these bands. This is carried out using octave bands with centre frequencies 125, 250 and 500 Hz and the decay curves are shown in Figure 4.5. Fitting straight lines to these curves, one will find that the time for the sound pressure level to decrease 60 dB is 1 second, which was input to the calculations using Equation (4.15). For simplicity, the decay curves are not calculated using the integration procedure given by Equation (4.2) but by a running short-time (50 milliseconds) integration of the squared response. In fact, such a procedure simulates the working of the old level recorders.

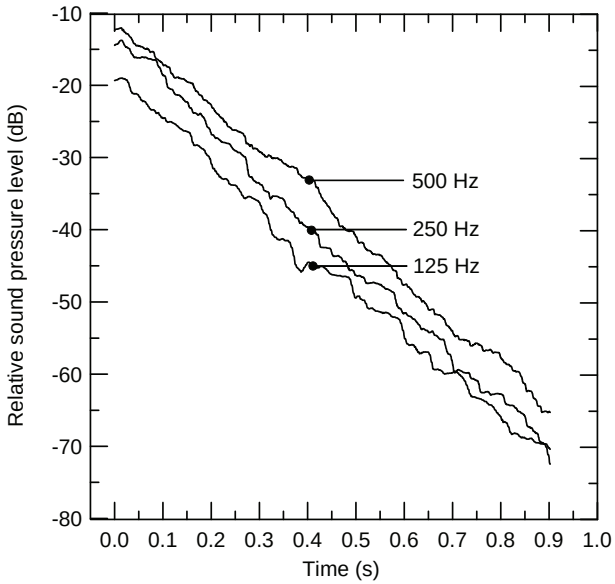

Figure 4.5 Decay curves in octave bands with centre frequencies 125, 250 and 500 Hz, calculated from the impulse response shown in Figure 4.4.

To conclude on this topic, we shall present examples of transfer functions based on impulse responses obtained in a real room like the one shown in Figure 4.1. The purpose is, for one thing, to show that transfer functions obtained in real rooms have the character as calculated and depicted in Figure 4.3. We shall use transfer functions based on impulse responses measured in the same auditorium as the one used for measuring the impulse response in Figure 4.1. The result is shown in Figure 4.6 where the sound pressure level (arbitrary reference) is given for the frequency range 100–200 Hz. One of these curves corresponds to the impulse response shown in Figure 4.1, for the other two curves the axis of the loudspeaker source is rotated 30° and 60°, respectively, from the horizontal plane. It goes without saying that the results exhibit the expected deterministic behaviour depending, among other factors, on the physical dimensions of the room.

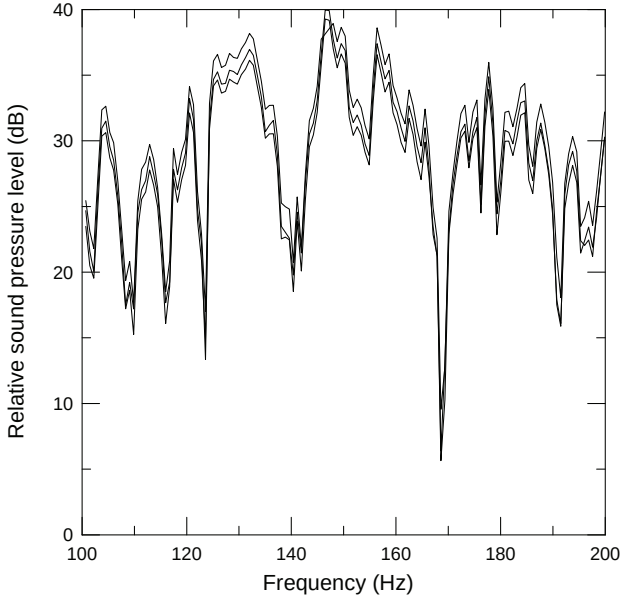

Figure 4.6 Some examples of transfer functions measured in an auditorium of volume 1800 m^3. Measurements by varying the direction of the loudspeaker axis.

4.5 STATISTICAL MODELS. DIFFUSE-FIELD MODELS

We demonstrated in section 4.4.2 that, rising to sufficiently high frequencies, one cannot link the various maxima in the transfer functions to the individual eigenfrequencies. These higher frequency maxima are the result of many, simultaneously excited modes adding up in phase. Correspondingly, minima in the response are the results of many modes having amplitudes and phase relationship resulting in a very small vector when added. It is also very important to realize that the general features of these transfer functions such as the distribution of minima, the level difference between minima and maxima, the phase change over a given frequency range etc. is not specifically dependent on the room or the relative position of the source and receiver. A "flat" frequency response curve, which is the aim when designing microphones and loudspeakers, will never be obtained in a room.

At sufficiently high frequencies, however, we may express the abovementioned variables by statistical means. Specifically, we shall be able to do this when the distance between the eigenfrequencies becomes less than the bandwidth of the resonances. The so-called *Schroeder cut-off frequency* f_S, given by

$$f_S = 2000\sqrt{\frac{T}{V}}, \tag{4.22}$$

where V and T are the volume (m^3) and reverberation time (s), respectively, may be used as a frequency limit above which a statistical treatment is feasible. This corresponds to a frequency where we will find approximately three eigenfrequencies within the bandwidth

of a resonance. The formula may be understood from the following facts: the resonance bandwidth is inversely proportional to the reverberation time and the separation between the eigenfrequencies is inversely proportional to the room volume. For the example used in Figure 4.3, we arrive at a cut-off frequency of approximately 250 Hz.

In building acoustics, however, we are not normally interested in a statistical description of pure tone responses for rooms. We shall look for responses averaged over frequency bands, octave or one-third-octave bands and broadband excitation sources are used. This leads to a treatment where we are looking at the energy or the energy density as the primary acoustic variable, which allows us to "forget about" the wave nature of the field as long as we keep away from the low frequency range. In this relation, it is pertinent to start by presenting a model that properly may be denoted the classical diffuse field model. It will appear that the formulae derived from this model are implemented in a number of measurement procedures both for laboratory and field use, in spite of their presumptions of an ideal diffuse field. An ideal diffuse field should imply that the energy density is everywhere the same in the room but, actually, acousticians have agreed neither on the definition nor on a measurements method for this concept. A couple of suggestions for a definition:

- In a diffuse field the probability of energy transport is the same in all directions and the energy angle of incidence on the room boundaries is random.
- A diffuse sound field contains a superposition of an infinite number of plane, progressive waves making all directions of propagation equally probable and their phase relationship are random at all room positions.

Both definitions, and a number of others, should be conceptually adequate but offer little help as to the design of a measurement method. We shall not delve into the various diffusivity measures being suggested, of which none has been generally accepted. In practice, when the international standards on laboratory measurements are concerned, procedures on improving the diffusivity are specified together with qualification procedures to be fulfilled before making the laboratory fit for a certain task. As for measurements in situ one is certainly forced to accept the existing situation.

In a number of standard measurement tasks in building acoustics, determination of sound absorption, sound insulation or source acoustic power, the primary tasks is to determine a time and space averaged squared sound pressure in addition to the reverberation time. In several cases, pressure measurements may be substituted by intensity measurements but still averaging procedures in time and over closed surfaces must be applied. Concerning the measurement accuracy of the averaged (squared) sound pressure and the reverberation time, this may be predicted using statistical models for the sound field. We shall return to this topic after treating the classical model for a diffuse sound field.

4.5.1 Classical diffuse-field model

For the energy balance in a room where a source is emitting a given power W (see Figure 4.7), a simple differential equation may be set up. This power is either "picked up", i.e. absorbed, by the boundary surfaces or other objects in the room or contributes to the build-up of the sound energy density. The boundary surfaces certainly include all absorbers which may be mounted there. We may write

$$W = \sum_j \left(W_{\text{abs}}\right)_j + V \cdot \frac{\mathrm{d}w}{\mathrm{d}t}, \tag{4.23}$$

where V is the room volume and w is the *energy density* (J/m^3) in the room. We shall, for simplicity, initially assume that the room boundaries are the only absorbing surfaces, thereby relating the first term to the absorption factors α_j of these surface areas S_j. Hence

$$\alpha_j = \frac{(W_{\text{abs}})_j}{(W_{\text{i}})_j} = \frac{(W_{\text{abs}})_j}{I_{\text{b}} \cdot S_j}, \tag{4.24}$$

where W_{i} is the power incident on all boundaries (walls, floor and ceiling) and I_{b} is the corresponding sound intensity.

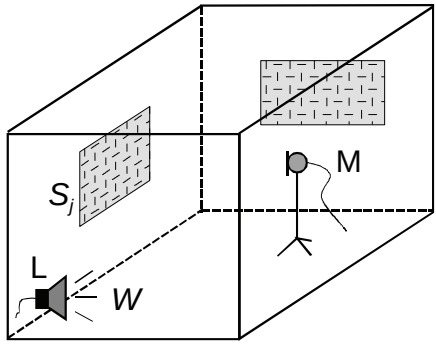

Figure 4.7 Room with a sound source, emitting a power W.

Having assumed that the energy density is everywhere the same implies that the latter quantities are independent of the position on the boundary. Equation (4.23) may therefore be written as

$$W = I_{\text{b}} \cdot \sum_j \alpha_j S_j + V \cdot \frac{\text{d}w}{\text{d}t} = I_{\text{b}} \cdot A + V \cdot \frac{\text{d}w}{\text{d}t}, \tag{4.25}$$

where A (m^2) is the total absorbing area of the room. It remains to find the relationship between the energy density w and the intensity I_{b}. It should be noted that the total sound intensity at any position in the room is ideally equal to zero because the energy transport is the same in all directions but certainly, we may associate an effective intensity with the energy transport in a given direction. The idea is then to calculate the part of the energy contained in a small element of volume that per unit time impinges on a small boundary surface element, thereafter integrating the contributions from the whole volume. We shall skip the details in this calculation, which results in

$$I_{\text{b}} = \frac{w \cdot c_0}{4} = \frac{\dfrac{\tilde{p}^2}{\rho_0 c_0^2} \cdot c_0}{4} = \frac{\tilde{p}^2}{4\rho_0 c_0}. \tag{4.26}$$

Additionally, we have introduced the relationship between the sound energy density and the sound pressure in a plane progressive wave, this due to our assumption that the sound

field in the sound is a superposition of plane waves. As seen from the formula, the intensity at the boundaries differs only by the constant 4, different from the corresponding one in a plane progressive wave. Introducing this result into Equation (4.25) we get

$$W = \frac{\tilde{p}^2}{4\rho_0 c_0} \cdot A + \frac{V}{\rho_0 c_0^2} \cdot \frac{\mathrm{d}\left(\tilde{p}^2\right)}{\mathrm{d}t}. \tag{4.27}$$

Obviously, the pressure root-mean-square value here must be interpreted as a short-time averaged variable, i.e. the averaging must be performed over a time interval much less than the reverberation time. The general solution of this equation is given by

$$\tilde{p}^2 = \frac{4\rho_0 c_0}{A} \cdot W + K \cdot \mathrm{e}^{-\frac{Ac_0}{4V}t}. \tag{4.28}$$

The constant K is determined by the initial conditions. We shall look into two special cases, applying this solution.

4.5.1.1 The build-up of the sound field. Sound power determination

We now assume that the sound pressure is zero when the source is turned on, ($\tilde{p} = 0$ at $t = 0$) , which gives

$$\begin{aligned} K &= -\frac{4\rho_0 c_0}{A} \cdot V \quad \text{and} \\ \tilde{p}^2 &= \frac{4\rho_0 c_0}{A} W \left(1 - \mathrm{e}^{-\frac{Ac_0}{4V}t} \right). \end{aligned} \tag{4.29}$$

The sound will then build up arriving at a stationary value when the time t goes to infinity. The RMS-value of the sound pressure becomes

$$\tilde{p}^2_{t\to\infty} = \frac{4\rho_0 c_0}{A} W. \tag{4.30}$$

The equation then gives us the possibility of determining the sound power emitted by a source by way of measuring the mean square pressure in a room having a known total absorbing area. For laboratories this type of room is called a *reverberation room* and procedures for such measurements are found in international standards (see e.g. ISO 3741).

A couple of important points concerning such measurements must be mentioned. As pointed out above, one has to determine the time and space averaged value of the sound pressure squared. This is accomplished either by measurements using a microphone (or an array of microphones) at a number of fixed positions in the room or by a microphone moved through a fixed path in the room (line, circle etc.). One must, however, avoid positions near to the boundaries where the sound pressure is systematically higher than in the inner parts of the room. Waterhouse (1955) has shown that the sound pressure level at a wall, at an edge and at a corner, respectively, will be 3,

6 and 9 dB higher than the average level in the room. This is also easily demonstrated by direct measurements. Restricting the determination of the average sound pressure level to the inner part of a room, normally half a wavelength away from the boundaries, implies that we are "losing" a part of the sound energy. One therefore finds that the standards include a frequency-dependent correction term, the so-called *Waterhouse correction* to compensate for this effect and the power is then calculated from

$$W = \frac{\tilde{p}_\infty^2}{4\rho_0 c_0} A\left(1+\frac{Sc_0}{8Vf}\right), \tag{4.31}$$

where S is the total surface area of the room. In addition, the standard ISO 3741 includes some minor corrections for the barometric pressure and temperature and furthermore, the absorption area A is substituted by the so-called *room constant* R where

$$R = \frac{A}{1-\frac{A}{S}} = \frac{A}{1-\bar{\alpha}}, \tag{4.32}$$

and where $\bar{\alpha}$ is the mean absorption factor of the room boundaries. Normally, the mean absorption factor is required to be small for laboratory reverberation rooms making this correction also small. However, in the high frequency range (above 8–10 kHz) this may not be the case, especially due to air absorption (see section 4.5.1.3).

4.5.1.2 Reverberation time

Turning off the sound source when the stationary condition is reached, i.e. setting $\tilde{p}^2(t) = \tilde{p}_\infty^2$ at time $t = 0$, and $W = 0$ for $t > 0$, we get

$$\tilde{p}^2(t) = \tilde{p}_\infty^2 \cdot \mathrm{e}^{-\frac{Ac_0}{4V}\cdot t}. \tag{4.33}$$

As the reverberation time T is defined by the time elapsed for the sound pressure level to decrease by 60 dB, or equivalent, that the sound energy density has decreased by a factor 10^{-6}, we write

$$\frac{\tilde{p}^2(T)}{\tilde{p}_\infty^2} = 10^{-6} = \mathrm{e}^{-\frac{Ac_0}{4V}\cdot T}, \tag{4.34}$$

which gives us the reverberation time, commonly denoted T_{60}, as

$$T_{60} = \ln\left(10^6\right)\cdot\frac{4V}{c_0 A} \approx \frac{55.26}{c_0}\cdot\frac{V}{A}. \tag{4.35}$$

This is the famous reverberation time formula by Sabine, which is the most commonly used in practice in spite of its simplicity and the assumptions lying behind its derivation. Obviously, it cannot be applied for rooms having a very high absorption area. Setting the absorption factor equal to 1.0 for all surfaces, we still get a finite reverberation time whereas it is obvious that we shall get no reverberation at all. Other formulae have been

developed taking account of the fact that the reverberation is not a continuous process but involves a stepwise reduction of the wave energy when hitting the boundary surfaces. We shall not go into detail but just refer to a couple of these formulae. The first one is denoted *Eyring's formula* (see Eyring (1930)), which may be expressed as

$$T_{\mathrm{Ey}} = \frac{55.26}{c_0} \cdot \frac{V}{-S \cdot \ln(1-\bar{\alpha})}, \tag{4.36}$$

where $\bar{\alpha}$ as before is the average absorption factor of the room boundaries, i.e.

$$\bar{\alpha} = \frac{1}{S} \sum_i \alpha_i S_i. \tag{4.37}$$

The formula is obviously correct for the case of totally absorbing surfaces as we then get T_{Ey} equal to zero. For the case of $\bar{\alpha} << 1$, the formula will be identical to the one by Sabine.

Still another is the *Millington–Sette formula* (Millington (1932) and Sette (1933)), where one does not form the average of the absorption factors as above but is using the average of the so-called absorption exponents $\alpha' = -\ln(1-\alpha)$. This leads to

$$T_{\mathrm{MS}} = \frac{55.26}{c_0} \cdot \frac{V}{-\sum_i S_i \ln(1-\alpha_i)}. \tag{4.38}$$

One drawback of this formula is that the reverberation time will be zero if a certain subsurface has an absorption factor equal to 1.0. In practice, the absorption factors α_i have to be interpreted as an average factor for e.g. a whole wall. It is claimed (see e.g. Dance and Shield (2000)) that when modelling the sound field in rooms having strongly absorbing surfaces this formula gives a better fit to measurement data than the formulae of Sabine and Eyring.

Sabine's formula is however widely used, also by the standard measurement procedure for determining the absorption area and absorption factors of absorbers of all types (see ISO 354). By the determination of absorption factors one measures the reverberation time before and after introduction of the test specimen, here assumed to be a plane surface of area S_{t}, into the room. The absorption factor is then given by

$$\alpha_{\mathrm{Sa}} = \frac{55.26 \cdot V}{c_0 S_{\mathrm{t}}} \left(\frac{1}{T} - \frac{1}{T_0} \right). \tag{4.39}$$

T_0 and T are the reverberation times without and with the test specimen present, respectively. One thereby neglects the absorption of the room surface covered by the test specimen but this surface is assumed to be a hard surface, normally concrete, having negligible absorption. We shall return to this measurement procedure in the following chapter.

To conclude this section, we mention that various extensions of the simple reverberation time formulae have been proposed, in particular to cover situations where the absorption is strongly non-uniformly distributed in the room. A review of these formulae may be found in Ducourneau and Planeau (2003), who performed an

experimental investigation in two different rooms comparing, altogether, seven different formulae. However, this number includes the three formulae presented above.

Here, we shall present just one example of the formulae particularly developed for covering the aspect of non-uniformity, a formula given by Arau-Puchades (1988). It applies strictly to rectangular rooms only and may be considered as a product sum of Eyring's formula defined for the room surfaces in the three main axis directions, *X*, *Y* and *Z*, each term weighted by the relative area in these directions. It may be expressed as

$$T_{\mathrm{AP}} = \left[q \cdot \frac{V}{-S \ln(1-\bar{\alpha}_X)} \right]^{\frac{S_X}{S}} \cdot \left[q \cdot \frac{V}{-S \ln(1-\bar{\alpha}_Y)} \right]^{\frac{S_Y}{S}} \cdot \left[q \cdot \frac{V}{-S \ln(1-\bar{\alpha}_Z)} \right]^{\frac{S_Z}{S}}, \quad (4.40)$$

where q is the factor $55.26/c_0$. Using this formula one may e.g. assign the area S_X to the ceiling and the floor having average absorption factor $\bar{\alpha}_{\mathrm{X}}$, the two sets of sidewalls to the corresponding surface areas and absorption coefficients with indices *Y* and *Z*. It will appear that this formula will predict quite longer reverberation times than predicted by the simple Eyring's formula in case of low absorption on the largest surfaces of the room.

4.5.1.3 The influence of air absorption

In the derivation of the formulae above we assumed that all energy losses were taking place at the boundaries of the room. This is only partly correct as one in larger rooms and/or at high frequencies one may have a significant contribution to the absorption caused by energy dissipation mechanisms in the air itself. This is partly caused by thermal and viscous phenomena but for sound propagation through air by far the most important effect is due to *relaxation* phenomena. This is related to exchange of vibration energy between the sound wave and the oxygen and nitrogen molecules; the molecules extract energy from the passing wave but release the energy after some delay. This delayed process leads to hysteretic energy losses, an excess attenuation of the wave added to other energy losses.

The relaxation process is critically dependent on the presence of water molecules, which implies that the excess attenuation, also strongly dependent on frequency, is a function of relative humidity and temperature. Numerical expressions are available (see ISO 9613–1) to calculate the attenuation coefficient, which include both the "classic" thermal/viscous part besides the one due to relaxation. The standard gives data that are given the title atmospheric absorption, as attenuation coefficient α in decibels per metre. This is convenient due to the common use of such data in predicting outdoor sound propagation. For applications in room acoustics, we shall, however, make use of the *power attenuation coefficient* with the symbol *m*, at the same time reserving the symbol α for the absorption factor. The conversion between these quantities is, as shown earlier, simple as we find

$$\alpha = \mathrm{Attenuation}\left(\mathrm{dB/m}\right) = 10 \cdot \lg(\mathrm{e}) \cdot m \approx 4.343 \cdot m. \quad (4.41)$$

Examples on data are shown in Figure 4.8, where the power attenuation coefficient *m* is given as a function of relative humidity at 20° Celsius, the frequency being the parameter.

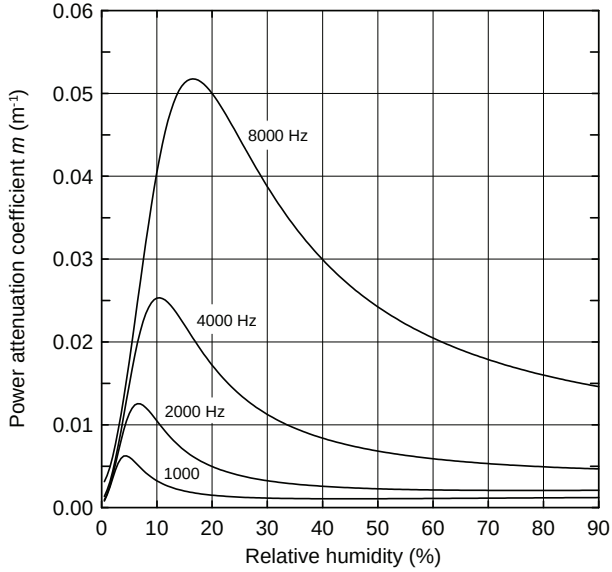

Figure 4.8 Power attenuation coefficient m for atmospheric absorption at 20° Celsius. Calculated from ISO 9613–1.

This atmospheric or air absorption brings about a modification of the total absorption area of a room by an added term $4mV$, where V is the volume of the room. Instead of Equation (4.35) we get

$$T_{60} = \frac{55.26}{c_0} \cdot \frac{V}{A_s + 4mV}, \tag{4.42}$$

where A_s represent the total absorption area in the room exclusive of the air absorption. This added term may certainly also be included in other expressions for the reverberation time by modifying the denominator in the Equations (4.36) and (4.38). (How should we include the air absorption into Equation (4.40)?). Certainly, the air absorption will be important in large rooms. However, at a relative humidity in the range 20–30 %, which is not unusual at certain times of the year in some countries, one will find that the reverberation time at frequencies above 6–8 kHz, even for moderate sized rooms, will be considerably influenced by air absorption.

Example In a room of volume 100 m^3 one measures a reverberation time of 0.5 seconds in the one-third-octave band with centre frequency 8000 Hz. The relative humidity is 20 %. Using Figure 4.8 we find that m is equal to 0.05 m^{-1} at the frequency 8000 Hz. (The figure applies to single frequencies but we shall use it to represent the corresponding frequency band.) The air absorption alone then gives an absorption area of 20 m^2. Applying Equation (4.35) we find the total absorption area A of the room is approximately 32.5 m^2. More than half of this absorption area is then due to air absorption. Without this contribution, the reverberation time would be well over one second.

Evidently, the air absorption may have important implications on the reverberation time but also on sound pressure levels in rooms at sufficiently high frequencies. We

referred in section 4.5.1.1 above to the standard ISO 3741 on sound power determination in a reverberation room, where a correction factor $(1-\bar{\alpha})$ was applied to the absorption area (see Equation (4.32)). Vorländer (1995) has shown that this correction factor is an approximation of the general term exp(*A*/*S*), where the absorption area is given by

$$A = -S \cdot \ln(1-\bar{\alpha}) + 4mV. \tag{4.43}$$

If *m* equals zero, we certainly arrive at the correction term in Equation (4.32) again as

$$\mathrm{e}^{-\frac{A}{S}} = \left[\mathrm{e}^{-\frac{-S\ln(1-\bar{\alpha})+4mV}{S}} \right]_{m=0} = 1-\bar{\alpha}. \tag{4.44}$$

Using this general correction, Vorländer (1995) obtains a very good fit, even up to 20 kHz, between the sound powers of a reference sound source determined in a reverberation room as compared with a free field determination.

4.5.1.4 Sound field composing direct and diffuse field

When deriving Equation (4.28), we assumed that the sound field was an ideal diffuse one; the energy density was everywhere the same in the room. It is obvious, however, that the source must represent a discontinuity; even in a room having a very long reverberation time there must exists a direct sound field in the neighbourhood of the source. We shall have to distinguish between the source near field, where the sound pressure may vary in a very complicated manner depending on the type of source, and the far field where the sound pressure decreases regularly with the distance from the source (see the discussion on sound sources in Chapter 3).

Assuming a position in the far field, we may apply the formula describing the relationship between the source sound power and the pressure squared in an ideal spherical (or plane) wave field:

$$W = \oint \frac{\tilde{p}^2}{\rho_0 c_0} \cdot \mathrm{d}S. \tag{4.45}$$

Initially, we shall assume that the source is a monopole, hence

$$\tilde{p}^2 = W \rho_0 c_0 \frac{1}{4\pi r^2}. \tag{4.46}$$

For other types of source, we may introduce a *directivity factor* D_θ, thus write

$$\tilde{p}^2 = W \rho_0 c_0 \frac{D_\theta}{4\pi r^2}, \tag{4.47}$$

where *r* is the distance from the source. The index θ on the directivity indicates that the latter generally depends on a properly defined angle. Combining this expression with the simple one giving the pressure in a diffuse field, Equation (4.30), we arrive at the following expression for the total sound field:

$$\tilde{p}_{\text{tot}}^2 = W\rho_0 c_0\left(\frac{D_\theta}{4\pi r^2}+\frac{4}{A}\right). \tag{4.48}$$

Expressed by the corresponding levels using standardized reference values for sound pressure and sound power, we may write

$$L_p = L_W + 10\cdot\lg\left(\frac{D_\theta}{4\pi r^2}+\frac{4}{A}\right). \tag{4.49}$$

For simplicity, we have given the characteristic impedance $\rho_0 c_0$ the value 400 Pa·s/m. The difference between the sound pressure level and the sound power level is shown in Figure 4.9 as a function of the relative distance $r/(D_\theta)^{1/2}$. The parameter on the curves is the absorption area A. The dashed curve indicates the relative level of the direct field.

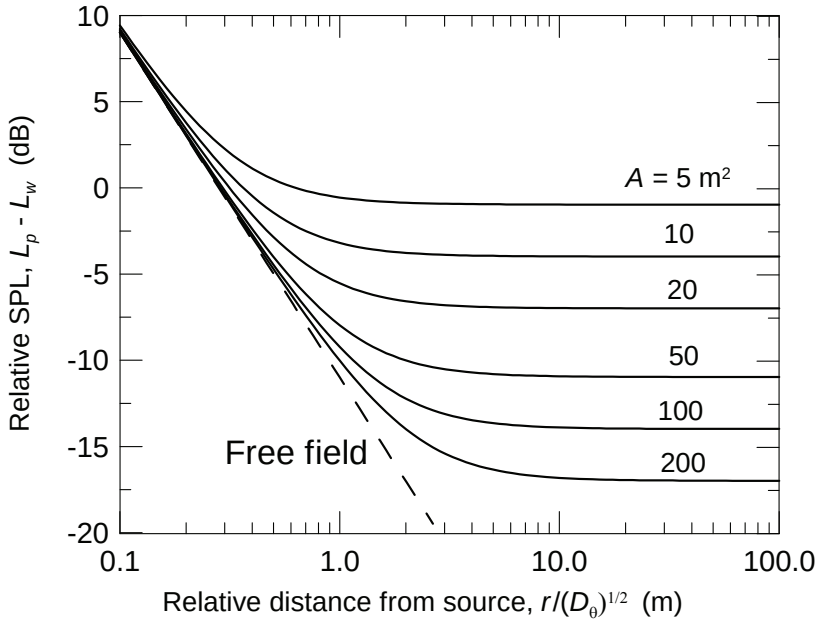

Figure 4.9 Sound pressure level as a function of relative distance from a source of sound power level L_W. The parameter is the room total absorption area A. The dashed line indicates the free field level.

The distance r_H from the source, where the contributions from the direct field and the diffuse field are equal, is called the *hall radius* or also *room radius* for the case where the directivity factor is equal to 1.0:

$$r_H = \sqrt{\frac{A}{16\pi}} = \sqrt{\frac{55.26}{16\pi c_0}\cdot\frac{V}{T}}. \tag{4.50}$$

Example In Figure 4.9 we calculated the difference between the sound pressure and the power levels for the cases where the absorption area varies between 5 and 200 m^2. Correspondingly, the room radius will vary between 0.32 and 1.99 metres.

4.5.2 Measurements of sound pressure levels and reverberation time

As pointed out in the introduction to section 4.5, the formulae derived using simple diffuse models are used in a number of measurement tasks both in the laboratory and in the field. Quantities such as sound pressure squared and reverberation time are considered, subject to certain presumptions, as global measures but in the sense of being average values with a space variance. We shall therefore have means to estimate this variance to be able to predict the uncertainty in the end results, results obtained by sampling the sound field in the room at a number of microphone positions.

Instead of sampling the sound field in a number of fixed positions, one may use a microphone moving continuously through the room. As the pressure is strongly correlated at adjacent positions, positions within some half a wavelength apart, implies that no new information is gained from close lying positions. The length of the path covered by such a microphone must therefore be carefully chosen by keeping this in mind. We shall return to this question later on, first, treating the case of using discrete sampling of the sound field to determine the average sound pressure squared and the reverberation time.

One may use several quantities to characterize the measurement uncertainty. It should also be noted that the expressions for the variance (or standard deviation) may be given as a relative value or not, which means that they are stated relative to the mean value or not. The relative variance of an actual quantity x shall be defined as

$$\sigma_{\mathrm{r}}^2(x) = \frac{\mathrm{E}\left\{\left(x - \mathrm{E}\{x\}\right)^2\right\}}{\mathrm{E}\{x\}^2}, \tag{4.51}$$

where the index r indicates a relative value and E{…} the expectation value. The square root of this expression is denoted the relative, sometimes the normalized, standard deviation. The symbol s is commonly used to indicate the standard deviation, indicating that practical calculations comprises a limited selection of data enabling us just to estimate the underlying expectation value.

4.5.2.1 Sound pressure level variance

An early effort to predict the space variance of the squared sound pressure is due to Lubman (1974), working on the determination of sound power level of sources in a reverberation room. At frequencies above the Schroeder cut-off frequency f_S (see Equation (4.22)) he found a relative variance of 1.0 for pure tone sources assuming that p^2 was exponentially distributed. The corresponding standard deviation $s(L_p)$ of the sound pressure level is then approximately equal to 5.6 dB, which implies that the 95% confidence interval will be as large as 22 dB. It should not come as a surprise that sound power level determination of pure tone sources present special problems in order to arrive at a reasonably correct space averaged value. Sources having a larger bandwidth will tend to “smear out” these space variations, thereby making the measurement task considerably easier. We shall present expressions below taking the bandwidth into account.

The Schroeder cut-off frequency represents an important division in the prediction of the variance. A satisfactory theory does not exist which covers the frequency range below this cut-off frequency. However, we shall present an estimate also for this range, a range where investigations are best conducted by FEM modelling. As for the frequency range above f_S, statistical models will have limited validity if the absorption becomes so large that the direct field is significant, which may happen at sufficiently high frequencies.

Lubman (1974) presented the following expressions for the relative variance:
For the range given by $0.2 \cdot f_S \le f \le 0.5 \cdot f_S$ he got

$$\sigma_r^2\left(p^2\right) = \frac{1}{1+\dfrac{\Delta N}{\pi}}, \tag{4.52}$$

where ΔN is the number of natural modes inside the frequency band Δf (see Equation (4.14)). As for the range $f \ge f_S$ he found

$$\sigma_r^2\left(p^2\right) = \frac{1}{1+\dfrac{\Delta f \cdot T}{6.9}}, \tag{4.53}$$

where T is the usual reverberation time. It should be noted that both expressions presuppose that the product $\Delta f \cdot T$ is numerically equal or larger than 20.

Normally, one is looking for the corresponding standard deviation $s(L_p)$ in the sound pressure level. However, to calculate this one needs to know the probability distribution of p^2. If the relative variance is less than approximately 0.5 we may make an estimate based on transforming the sound pressure level in the following manner:

$$L_p = 10 \cdot \lg\left(\frac{p^2}{p_0^2}\right) \tag{4.54}$$

$$\text{into} \qquad L_p = 10 \cdot \lg(\mathrm{e}) \cdot \ln(p^2) - 10 \cdot \lg\left(p_0^2\right) \approx 4.34 \cdot \ln(p^2) - 10 \cdot \lg\left(p_0^2\right).$$

Differentiating the last expression with regards to p^2, we get

$$\frac{\mathrm{d}\left(L_p\right)}{\mathrm{d}(p^2)} = 4.34 \cdot \frac{1}{p^2} \quad \text{or} \quad s\left(L_p\right) = 4.34 \cdot \frac{s\left(p^2\right)}{p^2} = 4.34 \cdot \sqrt{\sigma_r^2\left(p^2\right)}. \tag{4.55}$$

Up until now we have concentrated on the spatial variance. In measurements on stochastic signals there will also be a corresponding relative time variance given by

$$\sigma_t^2\left(p^2\right) = \frac{1}{\Delta f \cdot T_i}, \tag{4.56}$$

where T_i is the measuring or integration time used to determine p^2 in a given microphone position. Certainly, we are able to make this time variance arbitrarily small by extending the measuring time but there is, of course, a trade-off here. In practice, one normally

chooses a measurement time making the time variance some one-tenth of the expected spatial variance.

If the task is to determine the average stationary sound pressure level in a room set up by a given source, we may choose a number M of microphone positions. Assuming that the sound pressures at these positions are uncorrelated, i.e. the positions are some half a wavelength apart, we may estimate the relative variance in the mean value by the following equation

$$\sigma_{\mathrm{r}}^2\left(\overline{p^2}\right)=\frac{\sigma_{\mathrm{r}}^2\left(p^2\right)+\sigma_{\mathrm{t}}^2\left(p^2\right)}{M}, \qquad (4.57)$$

where we may insert the actual contributions to the variance from the Equations (4.52), (4.53) and (4.56).

The spatial variance expressions given above were developed in connection with the problem of sound power determination in reverberation rooms, i.e. a typical laboratory set-up in hard-walled rooms. They may, however, also be applied to field measurement such as sound insulation between dwellings, from which we shall give some examples taken from a NORDTEST report (see Olesen (1992)). The main content of this report may now be found in the standard ISO 140 Part 14.

In this report, however, some modifications are introduced in the above expressions when calculating the standard deviation $s(L_p)$. In Equation (4.52) the factor π is substituted by the number 8.5, which is claimed to give a better fit to experimental data. Furthermore, an additional term is introduced into Equation (4.53) allowing for a possible influence of the direct field from the source. Figures 4.10 and 4.11 show the results; the measured and the predicted standard deviation of the sound pressure level in two rooms having widely different volumes. Taking the valid range of the theoretical expressions into account, the fit between measured and predicted data are reasonably good. As for the smallest sized room, the expressions are not valid below approximately 150 Hz. For the larger room, there are also some discrepancies in the higher frequency range, most probably due to a relatively high and unevenly distributed absorption (carpeted floor). All results are based on measurements using five microphone positions for each of the two source positions used.

Apart from the determination of sound power of sources in reverberation rooms and the determination of sound insulation, great effort has been put into finding accurate methods for determination of sound pressure levels from service equipment in buildings. Service equipment noise normally involves low frequency components and small rooms makes a correct sampling of the room important, this is so even if legal requirements are commonly specified by the overall A- or C-weighted sound pressure levels. It has been shown (see e.g. Simmons (1997)) that combining a few microphone positions in the room with a corner position, the corner having the highest C-weighted sound pressure level, is an efficient procedure both with respect to the correct average value (less bias error) and to the reproducibility. This procedure has been adopted by the international standard ISO 16032.

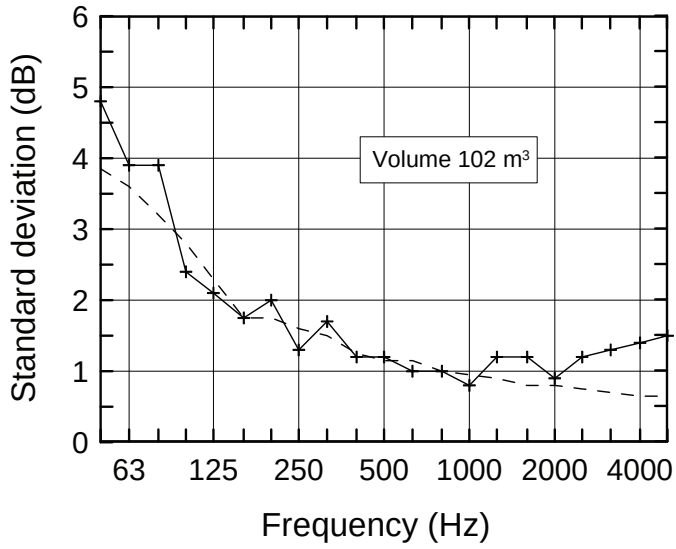

Figure 4.10 Spatial distribution of sound pressure level. Furnished living room with carpet, volume 102 m^3. Solid curve – measured standard deviation. Dashed curve – predicted standard deviation. After Olesen (1992).

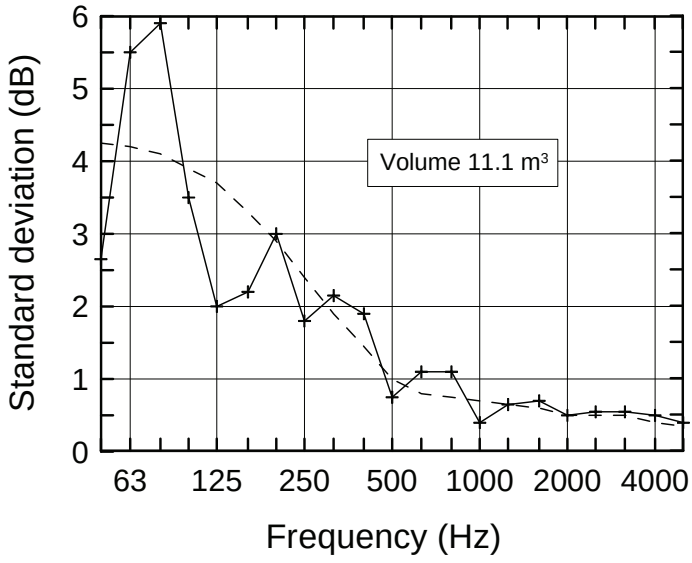

Figure 4.11 Spatial distribution of sound pressure level. Toilet with hard room boundaries, volume 11.1 m^3. Solid curve – measured standard deviation. Dashed curve – predicted standard deviation. After Olesen (1992).

4.5.2.2 Reverberation time variance

Measurements of sound decay and reverberation time in rooms are performed either by using a method based on an interrupted noise signal or by a method based on the integrated impulse response, specifically by

- exciting the room using a stochastic noise signal, usually filtered in octave or one-third-octave bands, and recording the sound pressure level after turning off the source, i.e. the method outlined when deriving the reverberation time formula in section 4.5.1.2
- measuring the impulse response, using either a maximum length sequence signal (MLS signal) or a swept sine signal (SS signal), which again is filtered in octave or one-third-octave bands, thereafter applying the method given in section 4.3.1.

As for the first method concerned one will, due to the stochastic noise of the signal, observe variations in the results when repeating the measurement. This will be the case even if both source and microphone positions are exactly the same. The reason is that the stochastic signal is stopped at an arbitrary time making the room excited by different "members" of the ensemble of noise signals produced by the source. It makes no difference if the stochastic signal in fact is pseudo stochastic, i.e. periodically repeats itself, as the source normally is not stopped coincident with this period. The variance due to the variation in the reverberation time measured at a given position we shall call an ensemble variance. This quantity $\sigma_e^2(T)$ is therefore an analogue of the time variance $\sigma_t^2(p^2)$ by a sound pressure measurement (see Equation (4.56)).

By measuring the reverberation time using M microphone positions, repeating each measurement N times in each position, the relative variance in the average reverberation will be given by

$$\sigma_r^2\left(\overline{T}\right) = \frac{\sigma_r^2(T) + \frac{\sigma_e^2}{N}}{M}, \tag{4.58}$$

where the first term is the variance due to the spatial variation. It should be noted that the last term will be zero when using an impulse response technique as the excitation signal will be deterministic in this case. This does not, however, imply that systematic errors cannot occur in this case if the system is not *time invariant*, e.g. due to temperature changes etc. during the measurement. The SS technique is less prone to such errors than the MLS technique.

Returning to the method of using interrupted noise, Davy et al. (1979) developed theoretical expressions for the two contributions to the variance, applicable to frequencies above the Schroeder frequency f_S. In effect, they calculated the variance of the slope of the decay curves but the results may easily be transformed to apply to the corresponding reverberation time. As expected, these expressions are functions of the filter bandwidth and reverberation time but also depends on the time constant (or "internal reverberation time") of the measuring apparatus together with the dynamic range available. It has to be remembered that at the time when this work was performed the equipment available was of analogue type such as the level recorder. We shall therefore just give an example applicable for one-third-octave measurements, using a dynamic range of 30 dB and a RC detector (exponential averaging). The time constant of this detector is assumed to be one-quarter of the equivalent time constant for the room. The relative variance of the mean reverberation time may then be written (Vigran (1980)) as

$$\sigma_{\mathrm{r}}^2\left(\overline{T}\right)=\frac{1.31+\dfrac{1.94}{N}}{f_0\overline{T}M}, \tag{4.59}$$

where f_0 is the centre frequency in the one-third-octave band. This expression is also used in the report by Olesen (1992) comparing with measurement results obtained in a small laboratory room of volume 65 m^3, having an almost frequency independent reverberation time of two seconds. The numbers N and M of source and microphone positions were two and six, respectively. The result is shown in Figure 4.12, given by the reverberation time standard deviation, i.e. by the expression

$$s(T)=\sigma_{\mathrm{r}}\left(\overline{T}\right)\cdot\overline{T}\cdot\sqrt{M}\ ,$$

and as seen, the fit between measured and predicted results is quite good.

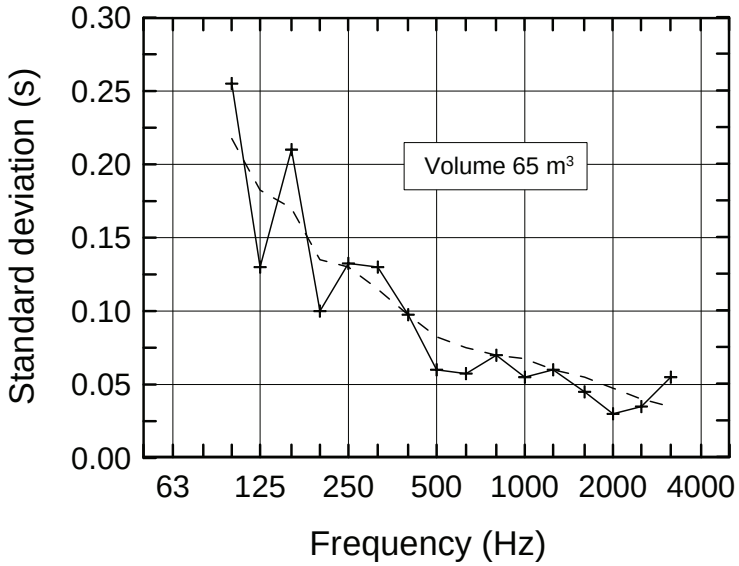

Figure 4.12 Reverberation time standard deviation in a laboratory room of volume 65 m^3. The reverberation time is approximately frequency independent (2 seconds). Solid curve – measured. Dashed curve – predicted. After Olesen (1992).

4.5.2.3 Procedures for measurements in stationary sound fields

As is apparent from the discussions above, a number of the standard measurement tasks in building acoustics; e.g. sound insulation, sound absorption and noise measurements, are based on determination of the spatial averaged sound pressure squared and the reverberation time. In the following, we shall use the sound pressure as an example.

We shall further assume that measurements are performed on band-limited stochastic noise. This may comprise measurements on a broadband source of unknown sound power where we apply filtering in octave or one-third-octave bands for the

analysis; e.g. in a sound power determination in a reverberation room. In other cases, we shall set up a sound field in a room with a loudspeaker driven by a narrowband signal. In the latter case, we may alternatively measure the impulse response (between the loudspeaker source signal and the signal from the microphone) using MLS or another deterministic signal. The latter procedure is certainly superior when the task is to determine *differences* in the squared sound pressures, e.g. when determining the airborne sound insulation between two rooms.

Regarding a spatial averaged value as a reasonably global one for the room presupposes that the room dimensions are of the same order of magnitude. This means that in those rooms where the dimensions are too different, a corridor, an open plan office or school, a factory hall etc., one will never, using a single source, find areas where the sound pressure level is constant (in the statistical sense of the word). We will experience a systematic variation; the sound pressure level will decrease more or less rapidly with the distance from the source depending on the room shape, the absorption and the presence of scattering objects. We shall return to this subject in section 4.9.

In most measurements standards, the required end result is the mean sound pressure level and quantities derived from it. The underlying quantity, however, is the mean squared pressure. In principle, we may proceed in two ways: We may sample the sound field in a number M of microphone positions, which we in fact assumed when deriving the expressions above, thereby calculating the mean sound pressure using the formula

$$\overline{L}_p = 10 \cdot \lg \left[\frac{\sum_{i=1}^{M} p_i^2}{M p_0^2} \right] \quad \text{(dB)}, \tag{4.60}$$

where p_i^2 denotes the time averaged squared pressure in position i. Alternatively, we may use a microphone moving along a certain path in the room, performing a continuous averaging process in time and space. We will then write

$$\overline{L}_p = 10 \cdot \lg \left[\frac{\frac{1}{T_{\text{path}}} \int_0^{T_{\text{path}}} p^2(t)\, dt}{p_0^2} \right] \quad \text{(dB)}, \tag{4.61}$$

where T_{path} is the time used for the complete path.

How do we compare these two methods as to the measuring accuracy? If a given length of the path could be attributed to a certain equivalent number M_{eq} of discrete positions we could apply the equations given in section 4.5.2.1 directly for the calculation of the standard deviation according to Equation (4.57). The time averaging term σ_t should not give any problem as the total measuring time is $T_{\text{path}} = T_i \cdot M$, but how long should the path be to correspond to M positions spaced at a distance ensuring uncorrelated sampling? This may be calculated for frequencies above the Schroeder frequency f_S and for a circular path, which is the most practical one, we approximately (perhaps not particularly surprising) get

$$M_{\mathrm{eq}}(\text{circular path}) \approx \frac{4\pi r}{\lambda} = \frac{4\pi r f_0}{c_0}. \qquad (4.62)$$

The quantities r and f_0 are the path radius and the centre frequency in the actual frequency band, respectively. A microphone path corresponding to three discrete microphone positions at 100 Hz should, therefore, have a radius of approximately 0.8 metres.

Accurate estimates of the measurement accuracy at frequencies below f_S are difficult to attain, but there are guidelines in measurement standards to improve the accuracy (see below). As seen from Equation (4.52), the number of modes excited is vital, and exciting the room by band-limited noise will certainly excite most modes inside the frequency band. However, we have seen that a source cannot excite a mode having a node at the source position. This is one reason for the requirements in standards to use several source positions, which is particularly important when measuring at low frequencies. It should not come as a surprise that some laboratories are, using not only a moving microphone but also a moving source.

Eventually, at sufficiently low frequencies, the number of modes will be too small to realistically speak of a space averaged value of the squared pressure. The exception is when the frequency gets so low that there will only be a homogeneous pressure field in the room, i.e. when going below the first eigenmode for the room.

Guidelines and help on these questions are given in national and/or international standards. These give guidance and requirements as to the choice of measuring positions and source positioning; the number of these depending i.a. on frequency and room volume, the distance of microphone positions from the source and from the room boundaries etc. Information is also given on the measurement uncertainty of the procedure or method. Concerning the latter, one will find the concepts of *repeatability* and *reproducibility* standard deviation. The former implies the standard deviation obtained when repeating a given procedure within a short time interval and under identical conditions (same laboratory, same operator, same measuring equipment). Otherwise, when these conditions are unequal, we have reproducibility conditions. The standard deviation of reproducibility therefore includes the standard deviation of repeatability. Data for reproducibility are usually established by round robin experiments by a number of participating laboratories.

To conclude, one will find the necessary instructions in the relevant standards to perform most measurement tasks. The purpose of dealing in some detail with the basis for these measurements are twofold: to give some understanding of the formulations, found in these standards, at the same time give some assistance when presented with a measurement task not covered by any standard.

4.6 GEOMETRICAL MODELS

A number of computer software programs, of which many are commercially available, are developed to predict sound propagation in large rooms, e.g. concert halls or large factory spaces. We shall not present any overview of the various programs or deal with specific published work where these programs are used but limit ourselves to give an outline of the principles behind the models. The majority of prediction models used for large rooms are based on geometrical acoustics, partly combined with statistical concepts to include scattering effects. Judged by the concepts found in the literature dealing with these prediction models, there may be some confusion as to the number of basic methods used. In effect, there are only two basic methods, the *ray-tracing method* and the *image-*

source method. The models implemented in software programs are, however, given special names depending on the specific algorithm used and furthermore, there exist *hybrid* types combining principles from ray-tracing and image-source modelling. A review on computer modelling of sound fields is given a journal special issue (see Naylor (1993)).

4.6.1 Ray-tracing models

A pioneering work on computer modelling using the ray-tracing method is from Krokstad et al. (1968). Calculation involving ray tracing is based on simulating a point source emitting a large number of "rays" evenly distributed per unit solid angle. Each ray then represents a given solid angle part of the spherical wave emitted from the source. The rays are "followed" on their way through the room, either through a sufficiently long time span or until they hit a surface defined as totally absorbing (see Figure 4.13). The seating area in, for example, a concert hall, is a surface of the latter type. What is a "sufficiently" long time if such a surface does not exist? Pragmatically, one may choose the time according to the energy left in the ray after a certain time interval but there are also implementations where the last surface point hit is defined as a new source, in its turn emitting the rest energy of the ray, contributing to the reverberant energy in the room.

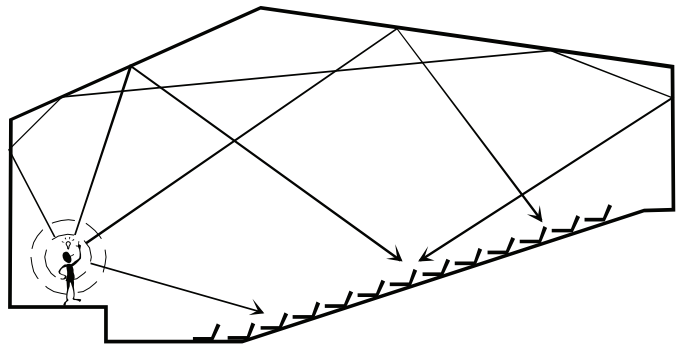

Figure 4.13 The principle of ray tracing.

A major problem using ray tracing is that a ray, per definition, has no extent, i.e. in practice it almost never hits a receiving point. This implies that the detectors ("microphones"), which shall record the rays hitting a given surface and thereby the magnitude and direction of the intensity, must be quite large. One may apply spherical microphones having a diameter in the range of one metre. Certainly, applying a very large number of rays, one may reduce the diameter but there is also the question of calculating time. There are alternative measures, such as using a beam having the shape of a cone of pyramid, but in effect, these are models of a hybrid type (see below).

One will also encounter the notion of "sound particle" instead of the ray and thereby the concept of sound particle tracing (see e.g. Stephenson (1990)). The algorithm to calculate the trajectories is the same; the sound particles or *phonons* propagate along rays. The differences are found on the receiving side; i.e. how the detectors are arranged and how the energy is calculated. In principle, however, it is still a ray-tracing method.

4.6.2 Image-source models

Image-source (or mirror-source) modelling is based on regarding all reflections from the boundary surfaces as sound contributions from images of the real source(s). The strength of this type of modelling, when carried out rigorously, is that it covers all transmission paths between source and receiver. It may give the impulse responses correct inside the framework of geometrical acoustics.

It is relatively simple mathematically to find all these mirror sources. The main problem is that except for rooms of very simple shapes, most of these sources are either not visible in a given receiver position or may be invisible in any part of, for example, the audience area. This means that a number of reflections are not physically valid. To separate out the "valid" image sources is a time-consuming task when coming to the higher order reflections. We may illustrate this by calculating the number of image sources of the order N in a room having M surfaces, which is given by $M(M-1)^{N-1}$. In a room having e.g. M equal to 12, we get approximately 16 000 image sources of the forth order, approximately 175 000 of the fifth order and so on. Except for rooms having a very simple shape, e.g. rectangular ones, maybe only a few hundred of these sources are valid. As in the case of ray tracing the question arises on when to stop the calculations. "Adding on" to the results using statistical arguments are common having carried out calculations correctly up to a given order of reflections.

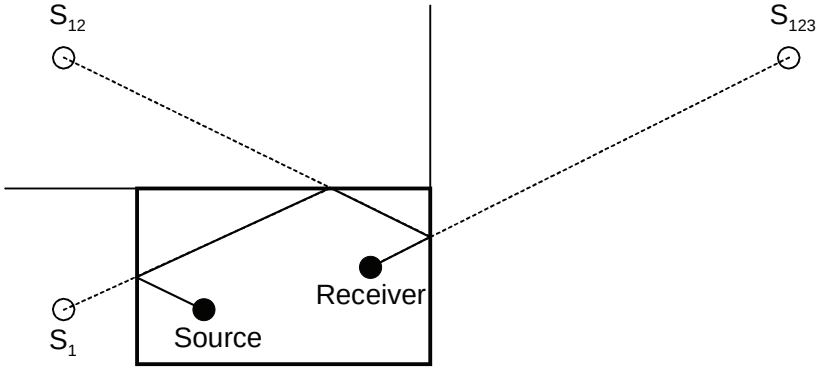

Figure 4.14 Example on trajectory between a receiver and a third-order image source.

Sketches which illustrate some of the aspects discussed above are shown in Figures 4.14 and 4.15. The first one shows, in a cross section (horizontally or vertically) through a room of rectangular shape (parallelepiped), an example of the trajectory between a receiver and a third-order image source. Figure 4.15 gives an example on a first-order image source S_1 (mirrored in wall W), which is not visible in any of the possible receiver positions R within the indicated sector, a sector given by the solid angle defined by the wall surface as seen from the image source.

Finding the image-source positions is in many cases quite easy where regular room shapes are concerned and one may also find analytical expressions as to the sound propagation. An example that we shall also use later on (see section 4.8) is sketched in Figure 4.16, which shows a vertical section of a long "flat" room. Here we shall assume that the ceiling height is much smaller than the other dimensions of the room; i.e. we shall neglect the influence of the sidewalls.

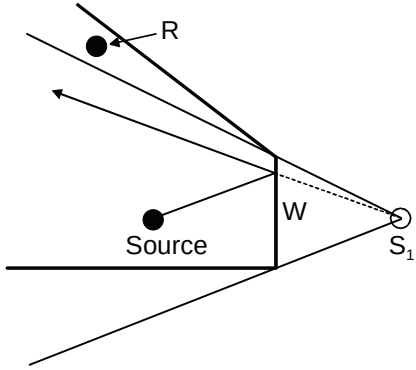

Figure 4.15 Example on image source not being visible in receiver positions *R*.

We shall put a source midway between the floor and the ceiling, initially assuming that the absorption factor α is the same for these boundary surfaces. The energy density w at a receiver position may then be expressed by

$$w = \frac{W}{4\pi c_0}\left[\frac{1}{r^2} + 2\sum_{n=1}^{\infty}\frac{(1-\alpha)^n}{r_n^2}\right], \qquad (4.63)$$

where W is the source sound power, r and r_n are the distances between the source and the receiver and between the receiver and the image source with index n, respectively.

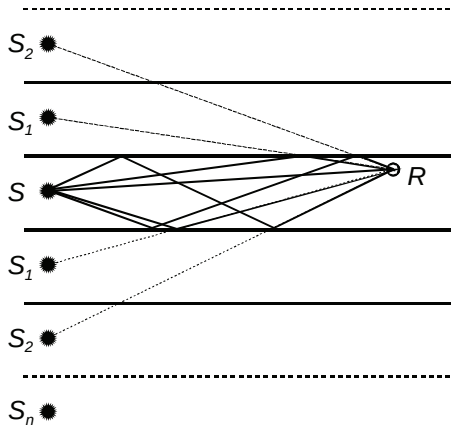

Figure 4.16 Image sources in a “flat” room.

4.6.3 Hybrid models

A number of the computer programs for room acoustic predictions are based on models that we may characterize as being hybrid; they comprise elements from ray-tracing methods as well as from image-source methods. An important aspect when developing such programs is to reduce the computing time.

A common practice is initially by finding available image sources by following ray trajectories, thereby noting the points on the boundaries hit by these rays. Thereafter, one is testing whether these reflection sequences will contribute to the energy in a given receiver position in the same manner as when using a pure image-source method. One makes use of a beam, either in the form of a cone or a pyramid, where the ray itself represents the axis. At each reflection, the highest point in the beam will represent an image source. This approach makes it possible to work with receivers represented by points, not as a large sphere necessary in a pure ray-tracing model. Certainly, the approach is not without its problems. The number of beams is certainly finite, making it possible to find only a limited number of image sources. Another problem is that the ray direction following a reflection is solely determined by the axis of the beam, which implies that the beam is not split up when it hits two or more surfaces. This makes it possible for some image sources to "illuminate" and thereby contribute to the energy in receiver points that in effect are not visible. And, vice versa, some image sources may not illuminate receivers that in fact should be visible. For a closer description of the procedure, see for example, Lewers (1993).

The necessary finite number of rays or beams will impose a limit on the accuracy of the calculated impulse response. One therefore has to apply other methods to add a reverberant "tail" to the response. This is coupled to the aspect of adding some diffuse reflections to the response. Obviously, scattering phenomena have strictly no place in geometrical acoustics but certainly being present in real rooms due to surface irregularities and objects filling the room. A strong element of diffuse reflections is also important in performance spaces such as concert halls etc., making it necessary by some artifice also to implement this aspect in the prediction models, mainly by some statistical type of reasoning.

4.7 SCATTERING OF SOUND ENERGY

With the concept of diffraction, it is generally understood that changes are taking place in the direction of sound propagation, thereby including both the concept of reflection and scattering. As to the former, one assumes that the dimensions of the reflecting surface are large as compared with the wavelength, the reflection is considered to be specular. The word scattering is commonly used when the dimensions of the surface or object hit are comparable or less than the wavelength. As pointed out above, scattering has strictly no place in geometrical acoustics. By e.g. ray-tracing modelling there is certainly no impediment for not making the reflection specular; the ray may be reflected in a random direction, however a physical reason for allowing such a diffuse reflection must exist.

Several hybrids models (see e.g. Heinz (1993); Naylor (1993b)) combine a strict calculation using specular reflections together with the addition of a certain number of such diffuse reflections. When modelling the sound field in large assembly halls, concert halls etc. one might say that the inclusion of diffuse energy is justified by the necessary partially detailed description of the room. In addition, scattering phenomena certainly exist when increasing the frequency and the wavelength is becoming comparable to the

size of objects. The energy in the incident wave will be redistributed with a directional distribution depending both on the shape of the object and on the ratio of wavelength to object dimensions.

Since 20 years ago, there has been a growing awareness that diffuse reflections are very important, especially for rooms for music performances. It is realized that an important contribution to the fame of some older concert halls, e.g. the Grosser Musikvereinsaal in Vienna, is the diffuseness provided by numerous surface irregularities: various types of surface decoration, columns, balconies etc. Following the work of Schroeder (1975, 1979) on the design of artificial diffusing elements based on number theory, a range of commercial as well as non-commercial diffusing elements are now in use in rooms for music production and reproduction. A comprehensible treatise may be found in Cox and D'Antonio (2004). Here we shall just give a short overview on these types of diffuser element. In this connection a series of measurement methods are developed to characterize the acoustic properties of such elements both in ISO (ISO 17497) and in AES (Audio Engineering Society).

4.7.1 Artificial diffusing elements

The sound scattering properties of solid bodies and surfaces is of great interest in many areas of acoustics and the distribution of the scattered energy around structures of various shapes for a given incident wave is well known. Such distributions are normally given in the form of a directivity pattern for the scattered wave. In room acoustic modelling, however, one is in most cases not interested in such a detailed pattern. A surface property of major interest is the total amount of non-specularly reflected sound energy in relation to the total reflected energy. In ISO 17497 Part 1 a quantity named the *scattering coefficient* s is defined,[1] as one minus the ratio of the specularly reflected acoustic energy E_{spec} to the total reflected acoustic energy E_{total}:

$$s = 1 - \frac{E_{\text{spec}}}{E_{\text{total}}}. \tag{4.64}$$

Theoretically, this quantity can take on values between zero and one, where zero means a totally specular reflecting surface and one means a totally scattering surface. Being measured in a reverberation room as a random incidence quantity in one-third-octave or octave bands, it represents a direct analogue to the statistical absorption factor.

The main purpose of the artificially diffusing elements is certainly to reduce the specularly reflected energy. However, from the point of view of the producers of such elements one would like to have a corresponding measure characterizing the uniformity of the reflected sound, in the same way as characterizing radiated sound from sources, e.g. loudspeakers. There seems as yet no universal agreement concerning such a *diffusion coefficient* (or *factor*) to characterize these so-called diffusers but there is ongoing work e.g. inside ISO. The problem is to arrive at a single number measure characterizing the scattering directivity pattern.

These artificial types of diffuser element constitute a hard surface with grooves or protrusions of various shapes. The surface irregularity used may be one-dimensional or two-dimensional, according to the task of making a diffuser working in one or two

[1] Having the unit of 1, it should have been termed *scattering factor*.

planes. We shall confine ourselves to the first type, as the extension to two dimensions is reasonably straightforward, conceptually at least.

Schroeder (1975) began his work on what we may term mathematical diffusers by investigating the scattering from surfaces shaped in the form of a maximum length sequence (MLS). We showed in section 1.5.2 the particular Fourier properties of these sequences giving a completely flat power spectrum. Then, quoting Schroeder: "Thus, because of the relation between the Fourier transform and the directivity pattern, a wall with reflection coefficients alternating between +1 and –1, would scatter an incident plane wave evenly (except for a dip in the specular direction which corresponds to the DC component in the spectrum)." The "MLS wall" was realized as a hard wall with "grooves" or wells a quarter of a wavelength deep in the area where a reflection factor of –1 was called for. In practice, such diffusers work, however, over a rather limited frequency range, approximately one octave. There are means of increasing the workable bandwidth, as recent research shows, but this implies adding active components to the diffuser (see Cox et al. (2006)).

However, there are other periodic sequences having useful Fourier properties, which make them excellently suited for modelling diffusing elements having a much broader bandwidth than the MLS. These are the *quadratic residue* sequences and the *primitive root* sequences (see e.g. Schroeder (1999), Cox and Antonio (2004)). The sequence forming the base for making a quadratic residue diffuser (QRD) is given by

$$s_n = m^2 \text{MOD } N \quad \text{where} \quad m = 1, 2, 3, \ldots \tag{4.65}$$

This means that s_n is the reminder when m^2 is divided by the prime number N. Taking N=7 as an example, we get the following sequence: 0, 1, 4, 2, 2, 4, 1. In a similar way as for the MLS diffuser the numbers are transformed into the corresponding depths d_n of the grooves or wells of the surface, but these are now not constant:

$$d_n = s_n \frac{d_{\max}}{(s_n)_{\max}}. \tag{4.66}$$

So how do we choose the maximum depth $d_{\max}$ and also the width of each well? Certainly, to make the diffuser work properly there should be plane wave propagation in each well and there must be a significant phase change for the waves reflected from the bottom. The design rule normally used for the latter, which determines the maximum workable wavelength or the equivalent minimum frequency, is expressed as:

$$d_n = \frac{s_n \lambda_{\max}}{2N} \qquad \text{or} \qquad f_{\min} = \frac{s_n c_0}{2N d_n}, \tag{4.67}$$

where c_0 is the speed of sound. This design rule implies that the mean depth of the wells at this frequency is of the order of a quarter of a wavelength. As for the width w of each well, we should ensure plane wave propagation, which implies being below the cut-off frequency giving

$$w = \frac{\lambda_{\min}}{2} \qquad \text{or} \qquad f_{\max} = \frac{c_0}{2w}. \tag{4.68}$$

The width w is normally chosen in the range of 5–10 cm. Making the wells too narrow may increase the surface area too much giving unwanted surface sound absorption, especially when the wells have separating walls (see Figure 4.17 a).

The other type of sequence having Fourier properties that makes them useful in the construction of broadband diffusers, giving little specular reflections, is the primitive root sequences. These are calculated in a slightly different way than the quadratic residue ones, given by:

$$s_n = p^n \text{MOD } N \quad \text{where } \text{n} = 1, 2, 3, \ldots \tag{4.69}$$

The number p is denoted a primitive root modulo N, also called a generating element because it generates a complete residue system in some permutation. As an example, choosing N equal to 7 there are two primitive roots, being 3 and 5. We shall use a higher number N in our example below, choosing N equal to 13 where the lowest primitive root is 2. Using (4.69) to calculate this sequence gives the values shown in Table 4.1.

Table 4.1 Primitive root sequence for N equal 13 and primitive root p equal 2. Well depths in mm for design frequency 1000 Hz.

n	1	2	3	4	5	6	7	8	9	10	11	12
s_n	2	4	8	3	6	12	11	9	5	10	7	1
d_n (mm)	28	57	113	43	85	170	156	128	71	142	99	14

In the last row the corresponding depths of the wells are given, calculated by equation (1.3) choosing a design frequency (f_{min}) of 1000 Hz. It should be noted that there is only N –1 cells in the sequence. As is apparent from the table and also from Figure 4.17, where we have put three such periods on a row, diffusers based on a primitive root sequence (PRD) are unsymmetrical.

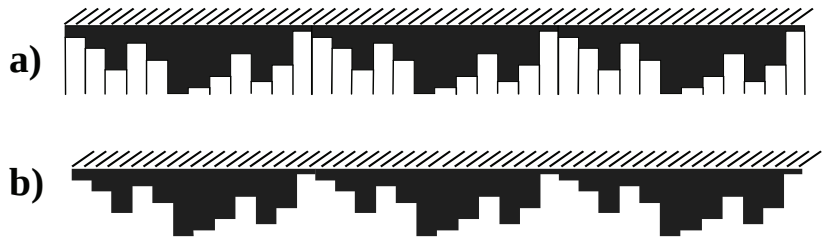

Figure 4.17 Sketch of a ceiling having three periods of a primitive root diffuser (PRD) with N equal 13.
a) With dividing walls between the wells (grooves), b) Without dividing walls.

Prediction methods for the acoustic pressure field, i.e. the sum of the direct field from a source and the scattered field, is normally based on the Helmholtz-Kirchhoff integral equation (see e.g. Cox and Lam (1994)). This means using Equation (3.44) in Chapter 3 with an added term representing the direct field. If only the far field is of interest, a computational method based on the analogue Fraunhofer diffraction method in

optics may be used. We shall not treat any of these methods here, but to illustrate the effect of these diffusers, especially to reduce the specular reflection, we shall present an example based on the FEM technique in two dimensions. The situation is depicted in Figure 4.18, showing the same three periods of the PRD depicted in Figure 4.17, where the wells (protrusions) are calculated in Table 4.1.

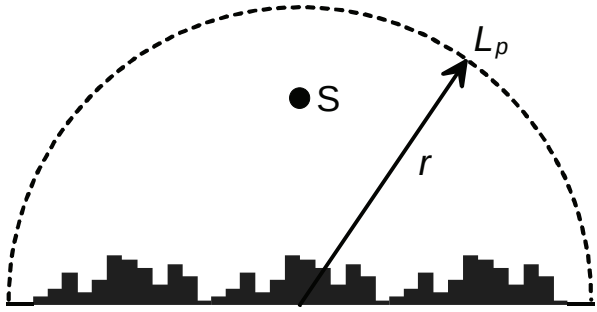

Figure 4.18 Sketch of situation for calculating the sound pressure level above a diffuser surface consisting of three periods of a primitive root sequence. Height of wells is given in Table 4.1 and height of point source (S) is 0.7 metres.

The resulting sound pressure level from a point source at height 0.7 metres is calculated on a circle with a radius of 1 metre above the diffuser. As the width of the wells is chosen equal to 5 cm, there will be a 10 cm flat (hard) surface added to each end of the diffuser. The calculations were performed using the Comsol Multiphysics™ software, modelling the field outside the semicircle to be a free field by adding a so-called perfectly matched layer (PML).

The results are shown in Figure 4.19, giving the total sound pressure level, at a design frequency of 1000 Hz, on the half-circle as a function of angle. The source acoustic power is arbitrarily set to 1 W, thus giving the rather high sound pressure levels. The FEM calculations are performed both for the situation described and also for a flat surface. The results are compared with a simple analytical calculation for an infinitely large flat surface. Apart from the discrepancies around the main lobe, the FEM calculations predict the flat surface situation quite well. The most important result, however, is the effect of the diffuser surface as compared by the flat one, giving a mean difference in the specular direction in the order of 6–8 dB.

4.7.2 Scattering by objects distributed in rooms

Big industrial halls, either production or assembly spaces, will always contain a large number of scattering objects. A realistic modelling of the sound propagation in such halls implies that one has to take scattering phenomena into account. Having objects covering a wide range of sizes, shapes and orientation in the room one certainly cannot take the influence of each object into account; one has to rely on rough characterizations and apply statistical concepts.

In presenting examples on calculating sound propagation in large rooms we shall use factory halls. It is therefore appropriate to give a short overview on the scattering theory used, which e.g. is outlined by Kuttruff (1981). Basically, two hypotheses are used:

- The sound scattering objects are assumed to be point like and the energy of the incident wave is scattered evenly in all directions.
- The scattering phenomenon follows a Poisson process. The energy emitted by the source is sent out in discrete quantities as "phonons" or sound packages having energy $W \cdot \Delta t$, where W is the sound power of the source.

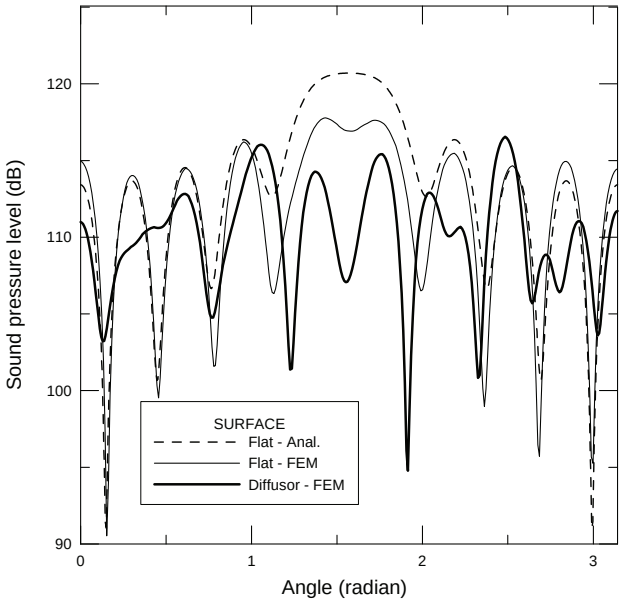

Figure 4.19 Total sound pressure level as a function of angle calculated on the circle with radius r equal one meter; situation as depicted in Figure 4.18. The source (S) power is equal to 1.0 W. Thick solid line – diffuser surface (FEM). Thin solid line – flat surface (FEM). Dashed line – flat, infinitely large surface (analytical).

The validity of the first hypothesis will depend on the ratio of the dimensions of the scattering object and the actual wavelength. Initially assuming that an object scatters sound, not only reflects sound in a specular way, we shall put up a limit on the relationship between a typical dimension D and the wavelength λ, demanding that $D/\lambda > 1/2\pi$.

From the second hypothesis follows that the probability density P_k of a phonon hitting a number k scattering objects within a time interval t_k is given by

$$P_k(c_0 t_k) = \frac{\mathrm{e}^{-qc_0 t_k} \cdot (qc_0 t_k)^k}{k!}, \tag{4.70}$$

where c_0 is the usual wave speed and q is the average *scattering cross section* per unit room volume, a quantity also denoted the scattering frequency.

The determination of q is difficult for scattering objects having a complicated shape. A common practice is equalizing the scattering effect (at high frequencies) of an object having a total surface area S by the one offered by a sphere of equal surface area. The average scattering cross section may then be expressed as

$$q = \frac{1}{V}\sum_{i=1}^{N}\frac{S_i}{4}, \tag{4.71}$$

when a total of N objects with surface areas S_i are present in a room of volume V.

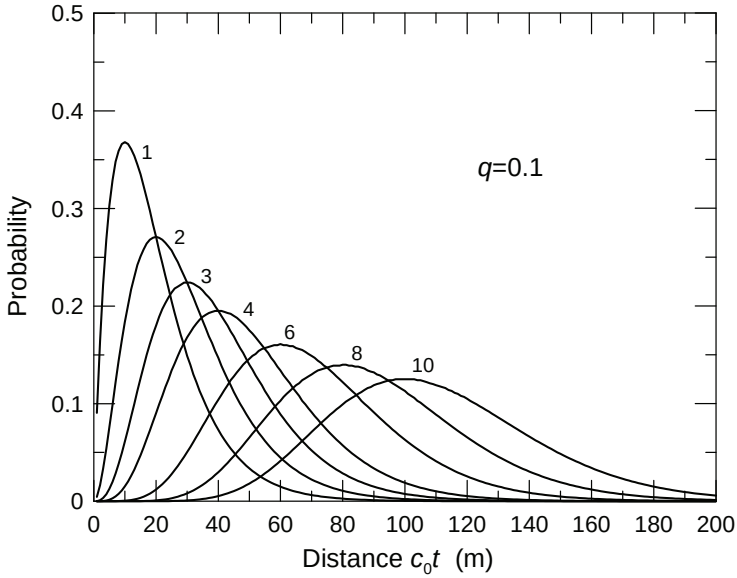

Figure 4.20 The probability of a wave (a phonon) hitting a given number of scattering objects, indicated by the number on the curves, having propagated a path of length $c_0 \cdot t$. The scattering cross section q is equal to 0.1m^{-1}.

Figure 4.20 shows the probability density P, according to Equation (4.70), of a phonon hitting a given number k of objects having propagated a path of length $c_0 \cdot t$. The number k is the parameter indicated on the curves calculated for a scattering cross section q equal to 0.1 m^{-1}. The Poisson distribution will typically give a high probability for hitting a single object; however, the corresponding width is small, whereas the probability for hitting many objects is small but the distribution is broad.

An important quantity relating to these aspects is the *mean free path* $\bar{R}$ of the sound. This quantity is generally used to characterize the path that the sound is expected to travel between two reflections. For an empty rectangular room having a volume V and a total surface area of S, we may show that $\bar{R}$ is equal to $4V/S$. Introducing scattering objects into the room (see Figure 4.21) we may, by using the probability function given by Equation (4.70), calculate the corresponding probability function of the free paths R and thereby the expected or mean value $\bar{R}$. The outcome is that $\bar{R}$ is equal to $1/q$.

4.8 CALCULATION MODELS. EXAMPLES

In the literature one will find reported a very large number of different models for predicting sound propagation in large rooms. A number of these are implemented in commercial computer software, e.g. CATT™, EASE™, EPIDAURE™ and ODEON™.

Most are developed for applications in performance rooms, i.e. for predicting the acoustics in rooms for speech and music. The trend is not only to give visual descriptions of the results but also to present the results by *auralization*. This implies that one may listen to music or speech "played" in a room at the design stage. This is accomplished by a process called *convolution*; the music or speech signal is convolved by the predicted impulse response belonging to a given source–receiver configuration.

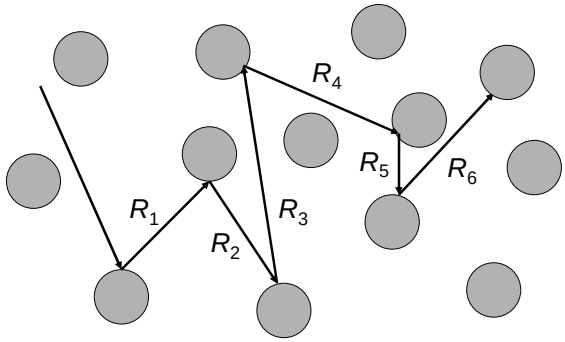

Figure 4.21 Sketch illustrating the concept of mean free path.

It is outside the scope of this book to give an overview or a closer description of this software based on the principles outlined in section 4.6. We shall, however, give examples on some special models primarily developed to predict sound propagation in large factory halls etc. The computer models mentioned above may certainly also be applied to such rooms but the ones we shall present cover the most important quantities to be predicted for such rooms: the attenuation of sound as a function of distance and the reverberation time. These are the analytical image-source models of Jovicic (1979) and Lindqvist (1982) together with the ray-tracing model of Ondet and Barbry (1989), the last including scattering in a very ingenious manner.

4.8.1 The model of Jovicic

The aim is to find an expression for the sound pressure level as a function of distance from a source of a given sound power level, which implies finding how the level decreases analogous to the results shown in Figure 4.9, however, without the constraint that the dimensions of the room should be fairly equal. Jovicic's models are confined to rooms of rectangular shapes, either "long" rooms, where one dimension is much larger than others (corridors etc.), or "flat" rooms, where two dimensions are much larger than the third one. We shall confine ourselves to the latter type, where the following assumptions are made:

- The influence of the sidewalls are neglected.
- The ceiling is treated as a plane surface like the floor. A serrated ceiling or ceilings with baffles etc. are treated as scattering objects.
- The absorption factor used is the mean value for the floor and ceiling.
- The sound source is placed midway between floor and ceiling.
- The scattering objects, which may also be assigned an absorption factor, are randomly distributed in the room.

The total energy density at a receiving point at a given distance r from the source is assumed to be given by

$$w_{tot} = w_d + w_s, \tag{4.72}$$

where w_d is the contribution from the direct sound, i.e. the non-scattered part, and w_s is the contribution from the phonons arriving at the receiver position after one or more collisions with the scattering objects. Without these scattering objects, w_d will be given by Equation (4.63) but now we shall have to modify this expression by subtracting the part being scattered or attenuated in other ways than by specular reflections from the room boundaries. We shall start looking at the scattered sound.

4.8.1.1 Scattered sound energy

Starting from the probability density given in Equation (4.70), Kuttruff (1981) calculated the corresponding probability that a phonon after a time t should be at a distance r from the source. In an infinite space, this probability density will be given by

$$P(r,t) = \left(\frac{3q}{4\pi c_0 t}\right)^{\frac{3}{2}} \cdot \mathrm{e}^{\frac{-3q}{4c_0 t} r^2}, \tag{4.73}$$

assuming that $qc_0t >> 1$, which implies that the travelled distance c_0t must be much larger than the mean free path $\bar{R} = 1/q$. It may also be mentioned that P is a solution of the so-called diffusion equation used in fluid dynamics, which is

$$\nabla^2 Q = \frac{1}{D} \cdot \frac{\partial Q}{\partial t}, \tag{4.74}$$

when setting the diffusion constant D equal to $c_0/(3q)$. The diffusion equation may e.g. describe how the concentration Q of a fluid, such as a dye, when injected into another fluid, changes with time. It should not be too difficult to envisage that this is a process quite analogous to how sound particles or phonons diffuse into a space containing scattering objects.

Jovicic assumes that the same probability $P(r,t)$ applies to the phonons from the image sources as all scattering objects are mirrored in the boundary surfaces (floor and ceiling) as well. The predicted total probability applicable to the phonons sent out from the original source and the image sources is then given by

$$P(r,t,h) = \frac{3q}{4\pi c_0 h t} \mathrm{e}^{\frac{-3q}{4c_0 t} \cdot r^2}, \tag{4.75}$$

where h is the height of the room. Inside a small volume element, containing the receiving position at a distance r from the source, we shall find phonons emitted from the source (and the image sources) at different points in time, thereby having different probability $P(r,t,h)$ of arriving at the chosen volume element. The shortest time of arrival will be r/c_0 and the longest one will be infinity.

On their way, the phonons are losing their energy, partly by hitting the scattering objects having absorption factor α_s, partly hitting the floor and ceiling having absorption factors α_f and α_c, respectively. In addition, we have the excess attenuation due to air

absorption characterized by the power attenuation coefficient m. All these attenuation processes may be assembled in a factor $\exp(-bc_0t)$, where b is a total attenuation coefficient comprising all loss mechanisms.

Now, the idea is to assume that this attenuation takes place gradually along the whole path covered by a phonon. Thereby, we may assemble all the energy of phonons arriving by calculating the integral

$$w_s = W \int_{r/c_0}^{\infty} P(r,t,h)\, e^{-bc_0 t}\, dt. \tag{4.76}$$

An approximate solution to this integral, where e.g. the lowest limit is zero, is given by

$$w_s = \frac{3qW}{2\pi c_0 h} K_0\left(r\sqrt{3qb}\right), \tag{4.77}$$

where K_0 is the modified Bessel function of zero order. The attenuation coefficient b may be expressed as

$$b = b'(\alpha', h, q) + \alpha_s q + m. \tag{4.78}$$

The quantity b', which expresses the attenuation due to the boundary surfaces is, as indicated, not only a function of the mean *absorption exponent* $\alpha' = -\ln(1-\alpha)$ for these surfaces but is also a function of the ceiling height and the scattering cross section.

4.8.1.2 "Direct" sound energy

The expression giving the direct energy density caused by the source and its infinite number of images (see Equation (4.63)) may approximately be solved by letting this row of sources be represented by a line source. The following solution is obtained:

$$w = \frac{WK}{2\pi r c_0 h} \cdot F_0\left(\frac{\alpha' r}{h}\right), \tag{4.79}$$

where

$$K = \frac{\alpha'}{2} \cdot \frac{2-\alpha}{\alpha} \qquad \text{with} \qquad \alpha' = -\ln(1-\alpha)$$

and

$$F_0(x) = \sin(x) \cdot \mathrm{Ci}(x) - \cos(x)\left[\mathrm{Si}(x) - \frac{\pi}{2}\right].$$

The functions Ci and Si are the so-called cosine and sine integral function (see e.g. Abramowitz and Stegun (1970)). We have thereby arrived at a closed expression for the energy density in the direct field but without taking the scattered part into account. We shall have to correct it by the probability $\exp(-qc_0t)$ that a phonon has *not* been scattered during the time t. Also taking the excess attenuation due to air absorption into account, we finally may express the direct (or the non-scattered) energy density by

$$w_{\mathrm{d}} = \frac{WK}{2\pi\, rc_0 h} \cdot \mathrm{F}_0\left(\frac{\alpha' r}{h}\right) \cdot \mathrm{e}^{-(q+m)r}. \qquad (4.80)$$

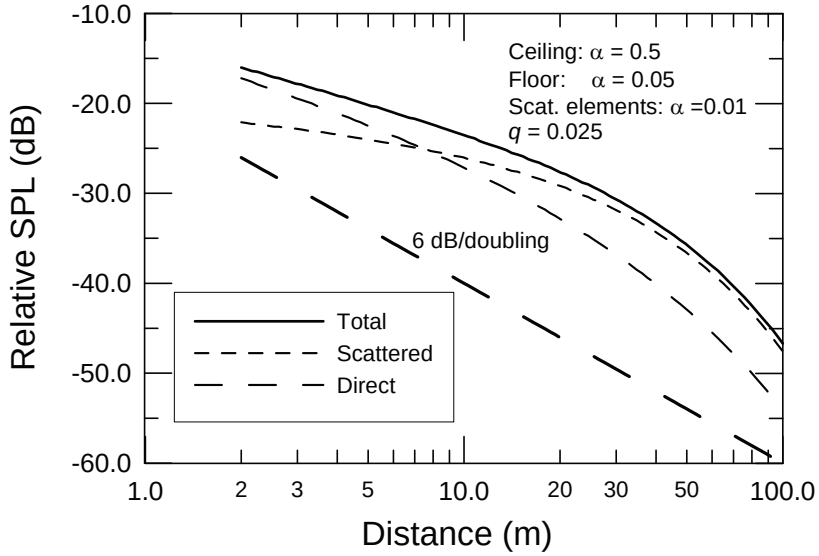

Figure 4.22 The relative sound pressure level as a function of distance from a source in a "flat" room. Contributions from scattered and non-scattered sound according to a model of Jovicic (1979). The room is 5 metres high.

4.8.1.3 Total energy density. Predicted results

The total energy density at a given distance from the source is then given by Equation (4.72) with w_{s} and w_{d} expressed by the Equations (4.77) and (4.80). We shall present some examples on using this equation where we, as in section 4.5.1.4, shall depict the relative sound pressure level, the difference between the sound pressure level L_p and the source sound power level L_w, as a function of the source–receiver distance. Assuming that the sound field is an assembly of plane waves having an intensity $w \cdot c_0$, we arrive at the ordinate for these curves by calculating the quantity $10 \cdot \lg(w \cdot c_0 / W)$.

The room height is chosen equal to 5 metres in all predictions shown. Furthermore, for simplicity the air absorption is put equal to zero. Figure 4.22 shows the total relative sound pressure level together with the separate contributions due to w_{d} and w_{s} for a room having a relatively small number of scattering objects; q is chosen equal to 0.025 m^{-1}. At large distances from the source, however, the level is still determined by the scattered field. For the sake of comparison, we have added a line representing the free field "distance law" for a monopole source, a 6 dB decrease per doubling of the distance. It should be obvious that one cannot apply any kind of "distance law", i.e. a constant number of decibels per distance doubling, in such rooms.

The next two figures show the total relative sound pressure level only but with different values for the absorption factor of the ceiling (see Figure 4.23) and in the mean scattering cross section q (see Figure 4.24). It should be noted that, even if the absorption exponents are entering into the equations above, the absorption factors α are used as input data when calculating the results.

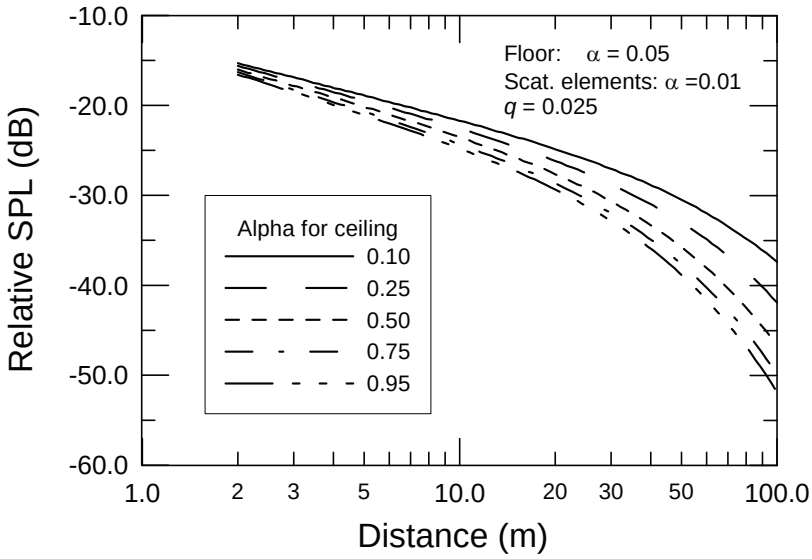

Figure 4.23 The relative sound pressure level as a function of distance from a source in a "flat" room. The room is 5 metres high. The parameter on the curves is the absorption factor α for the ceiling.

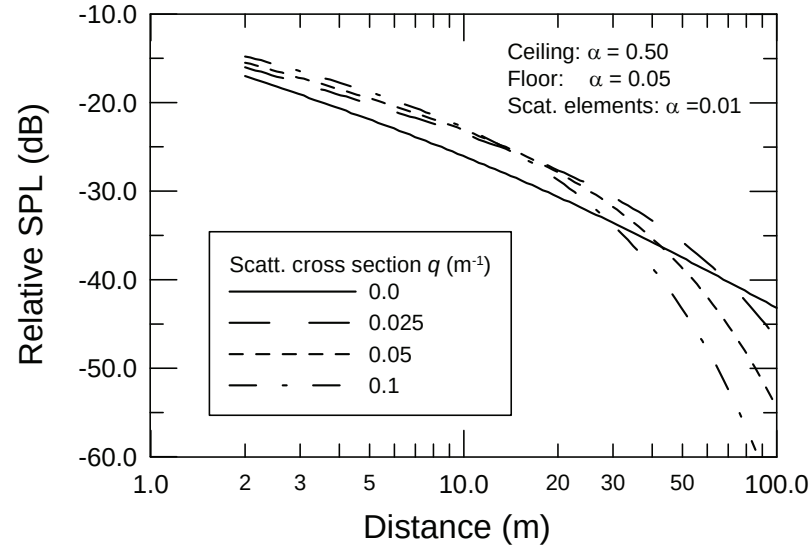

Figure 4.24 The relative sound pressure level as a function of distance from a source in a "flat" room. The room is 5 metres high. The parameter on the curves is the scattering cross section q (m^{-1}).

4.8.1.4 Reverberation time

Another effect to be observed in large rooms containing a large quantity of scattering objects is that the reverberation time is no longer a global quantity, but may vary systematically with the distance between source and receiver. This effect was observed by Jovicic (1971) by measurements in large industrial halls and confirmed theoretically by Vigran (1978) starting out from Jovicic's expressions given above.

The build-up of the scattered energy density in the room is given by Equation (4.76) As the build-up and the corresponding decay of sound energy are complimentary processes we may express the scattered energy density w_{rev} during decay as

$$w_{\mathrm{rev}} = w_{\mathrm{s}} - W \int_{r/c_0}^{t} P(r,t,h) \cdot \mathrm{e}^{-bt}\, \mathrm{d}t. \qquad (4.81)$$

Assuming that the mean scattering cross section q is relatively large, the scattered energy will dominate except when near to the source. In such a case we may use this equation directly to calculate the decay rate and thereby the reverberation time. A comparison between measured and predicted results is shown in Table 4.2. The reverberation time was measured by Jovicic (1971) in an industrial hall having a floor with dimensions 105 x 105 metres and a ceiling height of 11.5 metres. Measurements were performed in octave bands in the frequency range 125–4000 Hz at distances between source and receiver of 20 and 80 metre, respectively. The attenuation coefficient is given as a mean value, b equal to 1.22 m^{-1}, for this frequency range, and the mean scattering cross section q is stated to be 0.1 m^{-1}. The values in the table are average values for this frequency range and as seen, the fit between measured and predicted values are surprisingly good.

Table 4.2 Measured and predicted values for the mean reverberation time T at two different distances between source and receiver. Mean values for the frequency range 125–4000 Hz, in an industrial hall of volume 125 000 m^3.

Distance r (m)	Measured T (s)	Predicted T (s)
20	2.65	2.60
80	3.12	3.30

4.8.2 The model of Lindqvist

Lindqvist (1982) developed this analytically based image-source model further by also taking the reflections from the sidewalls into account, in addition, allowing for a random positioning of the source and receiver. The shape of the room is, however, still limited to rectangular, certainly a natural limitation for this kind of model. Based on the work of Kuttruff (see above), the scattering model applied by Lindqvist is more detailed than the one used by Jovicic but the scattering objects still have to be stochastically distributed in the room. The difference in predicted results using these two models will certainly depend on the actual situation. For relatively large rooms having not too much in the way of scattering object the differences is assumed to be relatively small, probably in the range of 1–2 dB.

In more recent time, the practical use of such analytical models is certainly reduced due to powerful computer simulations, either based on the ray-tracing or the image-source technique. The purpose of bringing forward the above works is primarily to illustrate some of the fundamental principles behind this type of modelling.

4.8.3 The model of Ondet and Barbry

An interesting solution to the problem of including scattering object was given by Ondet and Barbry (1989), which was implemented in the computer program RAYSCAT (RAYCUB in a later version). This is not, as the models discussed above, an image-source model but a ray-tracing one. Therefore, it does not impose any restrictions as to the shape of the room like the analytical models. The idea is to regard the areas of the room that contain scattering objects as zones having mean free paths depending on the density of these objects (see Figure 4.21). Each of these zones is allocated a certain mean free path $\overline{R} = R_k$, where the index k indicates the actual zone, whereas the areas without scattering object are allocated a mean free path $\overline{R} = \infty$. How is this idea compatible with a ray-tracing model where one certainly has to follow each ray around in the room?

Ondet and Barbry start by again using the Poisson distribution given by Equation (4.70), and they show that the paths lengths R_i covered between each hit have a probability density distribution given by

$$P(R) = q \cdot \mathrm{e}^{-qR}, \tag{4.82}$$

which gives an expected value $\mathrm{E}\{R\} = \overline{R} = 1/q$. Furthermore, one may generate these random distances R_i by using random numbers a_i between zero and one, thereafter inserting these numbers into the following expression:

$$R_i = -\overline{R} \cdot \ln(a_i). \tag{4.83}$$

The procedure is then as follows: One follows each ray in the normal manner until it crosses the border of a zone defined to contain scattering objects and thereby allocated a certain mean free path. A path length R_1 is then computed according to Equation (4.83) by drawing a random number a_1. This implies that it hits a scattering object after covering the distance R_1, thereafter directed in a random direction with a new random path length R_2. It may then hit another object within this zone or maybe escape from this zone.

A good fit between measured and predicted results is obtained by applying this procedure, both by Ondet and Barbry (1988) and others (see e.g. Vermeir (1992)). The computing time may, however, be quite long for rooms having complicated shapes, many zones with scattering objects of high density.

Later, other models have been developed (see e.g. Dance and Shield (1997)), limiting the room shape to rectangular where one may easily implement an image-source model, however, trying to keep the most important concepts from the Ondet–Barbry model; i.e. the subdivision of the room into zones containing scattering objects, the placement of absorbing element and barriers etc. The program CISM by Dance and Shield gives shorter computing times but at the expense of accuracy. It is not able to represent scattering in the same manner as the models treated above, which decreases the accuracy in areas far from the nearest source.

4.9 REFERENCES

ISO 9613–1: 1993, Acoustics – Attenuation of sound during propagation outdoors. Part 1: Calculation of the absorption of sound by the atmosphere.

ISO 3382: 1997, Acoustics – Measurement of the reverberation time of rooms with reference to other acoustical parameters. [Under revision to become ISO 3382 Acoustics – Measurement of room acoustic parameters. Part 1: Performance rooms; Part 2: Ordinary rooms.]

ISO 3741: 1999, Acoustics – Determination of sound power levels of noise sources using sound pressure – Precision methods for reverberation rooms.

ISO 354: 2003, Acoustics – Measurement of sound absorption in a reverberation room.

ISO 140–14: 2004, Acoustics – Measurement of sound insulation in buildings and of building elements. Part 14: Guidelines for special situations in the field.

ISO 16032: 2004, Acoustics – Measurement of sound pressure level from service equipment in buildings – Engineering method.

ISO/DIS 17497–1: 2002, Acoustics – Measurement of the sound scattering properties of surface. Part 1: Measurement of the random-incidence scattering coefficient in a reverberation room.

Abramowitz, M. and Stegun, I. A. (1970) *Handbook of mathematical functions*. Dover Publications Inc., New York.

Arau-Puchades, H. (1988) An improved reverberation formula. *Acustica*, 65, 163–180.

Cox, T. J., Avis, M. R. and Xiao, L. (2006) Maximum length sequences and Bessel diffusers using active technologies. *J. Sound and Vibration*, 289, 807–829.

Cox, T. J. and D'Antonio, P. (2004) *Acoustic absorbers and diffusers*. Spon Press, London and New York.

Cox, T. J. and Lam, Y. W. (1994) Prediction and evaluation of the scattering from quadratic residue diffusers. *J. Acoust. Soc. Am.*, 95, 297–305.

Dance, S. M. and Shield, B. M. (1997) The complete image-source method for the prediction of sound distribution in fitted non-diffuse spaces. *J. Sound and Vibration*, 201, 473–489.

Dance, S. M. and Shield, B. M. (2000) Modelling of sound fields in enclosed space with absorbent room surfaces. Part II. Absorptive panels. *Applied Acoustics*, 61, 373–384.

Davy, J. L., Dunn, I. P. and Dubout, P. (1979) The variance of decay rates in reverberation rooms. *Acustica*, 43, 12–25.

Ducourneau, J. and Planeau, V. (2003) The average absorption coefficient for enclosed spaces with non uniformly distributed absorption. *Applied Acoustics*, 64, 845–862.

Eyring, C. F. (1930) Reverberation time in "dead" rooms. *J. Acoust. Soc. Am.*, 1, 217–241.

Haas, H. (1951) Über den Einfluss eines Einfachechos auf die Hörsamkeit der Sprache. *Acustica*, 1, 49–58.

Heinz, R. (1993) Binaural room simulation based on an image source model with addition of statistical methods to include the diffuse sound scattering of walls and to predict the reverberant tail. *Applied Acoustics*, 38, 145–159.

Jovicic, S. (1971) Untersuchungen zur Vorausbestimmung des Schallpegels in Betriebgebäuden. Report No. 2151. Müller-BBN, Munich.

Jovicic, S. (1979) Anleitung zur Vorausbestimmung des Schallpegels in Betriebgebäuden. Report. Minister für Arbeit, Gesundheit und Soziales des Landes Nordrhein-Westfalen, Düsseldorf.

Krokstad, A., Strøm, S. and Sørsdal, S. (1968) Calculating the acoustical room response by the use of a ray tracing technique. *J. Sound and Vibration*, 8, 118–125.

Kuttruff, H. (1981) Sound decay in reverberation chambers with diffusing elements. *J. Acoust. Soc. Am.*, 69, 1716–1723.

Kuttruff, H. (1999) *Room acoustics*, 4th edn. Spon Press, London.

Lam, Y. W. (guest editor) (2000) Surface diffusion in room acoustics. *Applied Acoustics Special Issue*, 60, 2, 111–112.

Lewers, T. (1993) A combined beam tracing and radiant exchange computer model of room acoustics. *Applied Acoustics*, **38**, 161–178.

Lindqvist, E. (1982) Sound attenuation in factory spaces. *Acustica*, 50, 313–328.

Lubman, D. (1974) Precision of reverberant sound power measurements. *J. Acoust. Soc. Am.*, 56, 523–533.

Lundeby, A., Vigran, T. E., Bietz, H. and Vorländer, M. (1995) Uncertainties of measurements in room acoustics. *Acustica*, 81, 344–355.

Millington, G. (1932) A modified formula for reverberation. *J. Acoust. Soc. Am.*, 4, 69–82.

Naylor, G. (guest editor) (1993a) Computer modelling and auralisation of sound fields in rooms. *Applied Acoustics Special Issue*, 38, 2–4, 131–143.

Naylor, G. (1993b) ODEON – Another hybrid room acoustical model. *Applied Acoustics*, 38, 131–143.

Olesen, H. S. (1992) Measurements of the acoustical properties of buildings – Additional guidelines. *Nordtest Technical Report 203.*

Ondet, A. M. and Barbry, J. L. (1988) Sound propagation in fitted rooms – Comparison of different models. *J. Sound and Vibration*, 125, 137–149.

Ondet, A. M. and Barbry, J. L. (1989) Modelling of sound propagation in fitted workshop using ray tracing. *J. Acoust. Soc. Am.*, 85, 787–796.

Pierce, A. D. (1989) *Acoustics. An introduction to its physical principles and applications*. Published by the Acoustical Society of America through the American Institute of Physics, Melville, NY.

Schroeder, M. R. (1975) Diffuse sound reflection by maximum-length sequences. *J. Acoust. Soc. Am.*, 57, 149–150.

Schroeder, M. R. (1979) Binaural dissimilarity and optimum ceilings for concert halls: More lateral diffusion. *J. Acoust. Soc. Am.*, 65, 958–963.

Schroeder, M. R. (1999) *Number theory in science and communication*. Springer-Verlag, Berlin.

Sette, W. J. (1933) A new reverberation time formula. *J. Acoust. Soc. Am.*, 4, 193–210.

Simmons, C. (1997) Measurements of sound pressure levels at low frequencies in rooms. SP Report 1997: 27. SP Swedish National Testing and Research Institute, Borås, Sweden. (NORDTEST Project No. 1347-97.)

Stephenson, U. (1990) Comparison of the mirror image source method and the sound particle simulation method. *Applied Acoustics*, 29, 35–72.

Vermeir, G. (1992) Prediction of the sound field in industrial spaces. *Proceedings Internoise* 92, 727–730.

Vigran, T. E. (1978) Reverberation time in large industrial halls. *J. Sound and Vibration*, 56, 151–153.

Vigran, T. E. (1980) Corner microphone in laboratory rooms – Applicability and limitations (in Norwegian). *ELAB Report STF A80050.* NTH, Trondheim. (NORDTEST Project No. 129-78.)

Vigran, T. E., Lundeby, A. and Sørsdal, S. (1995) A versatile 2-channel MLS measuring system. Proceedings of the 15th ICA, 171–174, Trondheim, Norway.

Vorländer, M. (1995) Revised relation between the sound power and the average sound pressure level in rooms and consequences for acoustic measurements. *Acustica*, 81, 332–343.

Waterhouse, R. V. (1955) Interference patterns in reverberant sound fields. *J. Acoust. Soc. Am.*, 27, 247–258.